Activated regulatory T cells are the major T cell type emigrating from the skin during a cutaneous immune response in mice

Michio Tomura,[1] Tetsuya Honda,[2] Hideaki Tanizaki,[2] Atsushi Otsuka,[2] Gyohei Egawa,[2,3] Yoshiki Tokura,[4] Herman Waldmann,[5] Shohei Hori,[6] Jason G. Cyster,[7] Takeshi Watanabe,[3] Yoshiki Miyachi,[2] Osami Kanagawa,[1] and Kenji Kabashima[2,3]

[1]Laboratory for Autoimmune Regulation, Research Center for Allergy and Immunology, RIKEN, Yokohama City, Japan. [2]Department of Dermatology and [3]Center for Innovation in Immunoregulative Technology and Therapeutics, Kyoto University Graduate School of Medicine, Japan. [4]Department of Dermatology, University of Occupational and Environmental Health, Kitakyushu, Japan. [5]Sir William Dunn School of Pathology, Oxford, United Kingdom. [6]Research Unit for Immune Homeostasis, Research Center for Allergy and Immunology, RIKEN. [7]Howard Hughes Medical Institute and Department of Microbiology and Immunology, UCSF, San Francisco, California.

(1. AUTHOR: All abstracts and titles are reviewed by the JCI editors, and, when appropriate, substantial changes are made to ensure clarity and accessibility to our wide readership. Carefully read the title and abstract to ensure your meaning has been retained.)

(2. AUTHOR: Affiliations have been revised/renumbered to conform to JCI style; check for accuracy.)

(3. AUTHOR: Gene names and symbols have been edited according to JCI guidelines—see "Gene nomenclature and style" in the cover letter to this proof. Check for accuracy and indicate any other necessary changes.)

Tregs play an important role in protecting the skin from autoimmune attack. However, the extent of Treg trafficking between the skin and draining lymph nodes (DLNs) is unknown. We set out to investigate this using mice engineered to express the photoconvertible fluorescence protein Kaede, which changes from green to red when exposed to violet light. By exposing the skin of Kaede-transgenic mice to violet light, we were able to label T cells in the periphery under physiological conditions with Kaede-red and demonstrated that both memory phenotype $CD4^+Foxp3^-$ non-Tregs and $CD4^+Foxp3^+$ Tregs migrated from the skin to DLNs in the steady state. During cutaneous immune responses, Tregs constituted the major emigrants and inhibited immune responses more robustly than did LN-resident Tregs. We consistently observed that cutaneous immune responses were prolonged by depletion of endogenous Tregs in vivo. In addition, the circulating Tregs specifically included activated $CD25^{hi}$ Tregs that demonstrated a strong inhibitory function. Together, our results suggest that Tregs in circulation infiltrate the periphery, traffic to DLNs, and then recirculate back to the skin, contributing to the downregulation of cutaneous immune responses.

Introduction

Lymphocytes travel throughout the body to conduct immune surveillance. $CD4^+$ helper T cells are central organizers in immune responses. Upon stimulation, naive $CD4^+$ T cells differentiate into effector Th cells (1). $Foxp3^+$ Tregs represent a unique subpopulation of $CD4^+$ T cells that are important for maintenance of immunological homeostasis and self tolerance (2, 3). Naive T cells circulate between blood and secondary lymphoid tissues (4–7). However, it is debatable whether T cells travel through uninflamed peripheral tissues as part of their recirculation route. One type of peripheral tissue with the active afferent limb of the lymphatic system is, for example, the skin, and memory/effector T cells migrate to inflamed skin using CCR4 and CCR10 (8–10). Classic studies employing cannulation of afferent lymph vessels have shown that $CD4^+$ memory/effector cells make up nearly all cells in the afferent lymph of sheep (6, 11–13). On the other hand, Debes et al. have reported that $CD4^+$ cells, especially naive subsets, migrate from the skin in a CCR7-dependent manner using subcutaneous injection of fluorescent-labeled lymphocytes (14). However, the above experiments require traumatic or artificial procedures to follow or label T cells. Therefore, it is of interest to clarify whether T cells in the peripheral organs such as the skin migrate to draining LNs (DLNs) and to identify the T cell subsets of migration and their roles under physiological conditions.

To directly assess cells migrating from the peripheral tissue, we have devised a new experimental system that involves labeling resident cells using Tg mice expressing the Kaede protein. Kaede is a photoconvertible green fluorescence protein cloned from stony coral (15, 16) that changes its color from green to red when exposed to violet light (16). Therefore, the Kaede-Tg mouse system is an ideal tool for monitoring precise cellular movements in vivo at different stages of the immune response (17).

Here, we used the skin as a representative of the peripheral organs and observed the movement of cells from the skin using Kaede-Tg mice (17). A high proportion of the migrating cells into the DLNs were Tregs that had a stronger capacity to suppress acquired immune responses than LN-resident Tregs. Moreover, these migrating T cells recirculated into the skin upon elicitation to terminate immune responses.

Authorship note: Michio Tomura and Tetsuya Honda contributed equally to this work.

Conflict of interest: The authors have declared that no conflict of interest exists.

Citation for this article: *J Clin Invest.* 2010;120(3):xxxx–yyyy. doi:10.1172/JCI40926.

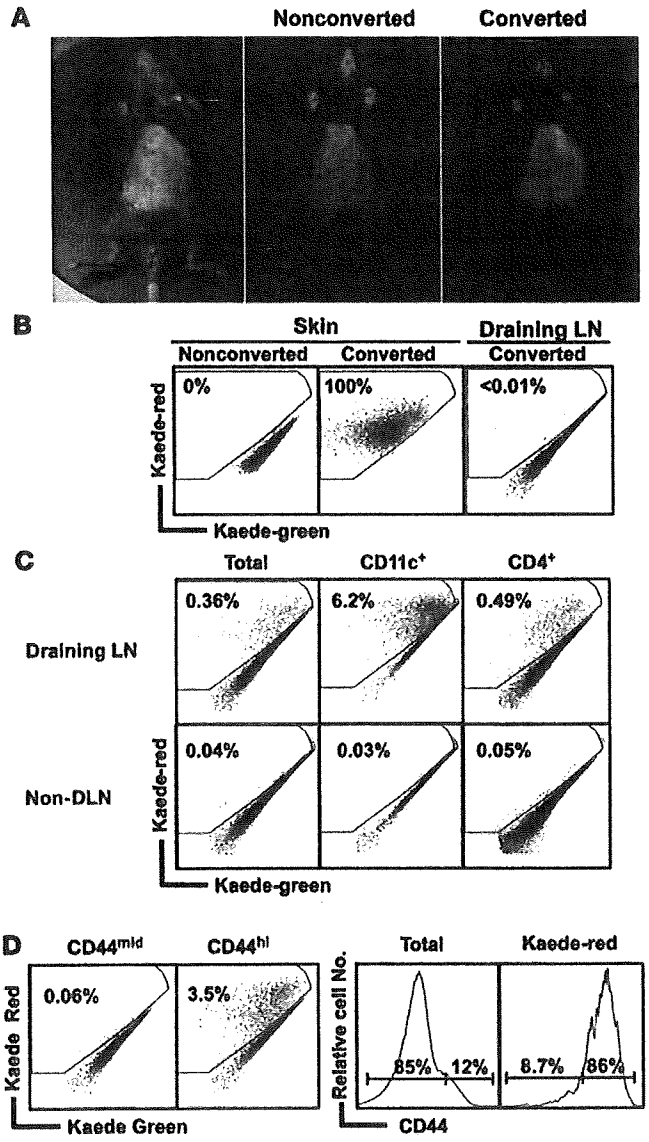

Figure 1

(11. AUTHOR: Please review gene names and abbreviations per Query 3 in all figures and in all figure legends.) Cell migration from the skin to the DLN in the steady state. (**A**) Kaede-Tg mice were photoconverted on the clipped abdominal skin as described in Methods and observed with a fluorescence stereoscopic microscope. Nonphotoconverted clipped skin is shown as a control (middle). Note: nonclipped area remains black since light cannot reach. (**B**) Skin and draining axillary LN cells resected immediately after violet light exposure of the abdominal skin and resected skin cells not exposed to violet light were subjected to flow cytometric analysis to evaluate the photoconversion. (**C** and **D**) Twenty-four hours after photoconversion of the abdominal skin, cells from the draining axillary and other nondraining cervical and popliteal peripheral LNs were stained with CD11c and CD4 mAbs (**C**) and CD4 and CD44 mAbs (**D**) and subjected to flow cytometry. These data are representative of at least 5 experiments. Numbers within plots or histograms (**B–D**) indicate percentage of cells in the respective areas.

Results

Detection of cell migration from the skin in the steady state using Kaede-Tg mice. To monitor cell migration from the skin in vivo, the abdominal skin of Kaede-Tg mice was photoconverted by exposure to violet light for 10 minutes (see Methods). Before photoconversion, all the cells in the skin of Kaede-Tg mice expressed only Kaede-green fluorescence (Kaede-green) (Figure 1, A and B). Immediately after violet light exposure to the skin, the whole skin tissue (Supplemental Figure 1; supplemental material available online with this article; doi:10.1172/JCI40926DS1) and the skin cells of the photoconverted area showed red signal (Kaede-red), whereas virtually no draining axillary LN cells (Figure 1, A and B, and Supplemental Figure 2) or blood cells (Supplemental Figure 2) were photoconverted. Although we found that Kaede-red proteins could be detected in the extracellular fluids when incubated for 24 hours after photoconversion of the LN cells (Supplemental Figure 3), we confirmed that the extracellular photoconverted Kaede proteins could not be transferred into T cells in vitro (Supplemental Figure 4).

To evaluate cell migration from the skin in the steady state, the clipped abdominal skin of Kaede-Tg mice was exposed to violet light as in Figure 1A, and 24 hours later, the draining axillary and nondraining cervical and popliteal LN cells were subjected to flow cytometry. We found that 0.36% of the DLN cells showed the Kaede-red phenotype (Figure 1C), suggesting a fraction of cells in the skin migrate to the DLNs. It is generally thought that dendritic cells are the major migrants from the skin in the steady state, and in fact 6.2% of $CD11c^+$ dendritic cells were of the Kaede-red phenotype in the DLNs (Figure 1C). In contrast, almost no Kaede-red $CD11c^+$ dendritic cells were detected in the non-DLNs (Figure 1C). We next evaluated $CD4^+$ T cell migration from the skin and found that 0.49% of $CD3^+CD4^+$ T cells in the DLNs had the Kaede-red phenotype (Figure 1C). Although the frequencies of the Kaede-red positivity among dendritic cells and $CD3^+CD4^+$ T cells differed, the absolute numbers of Kaede-red dendritic cells and $CD4^+$ T cells were comparable ($CD4^+$ T cells vs. $CD11c^+$ dendritic cells: 11621 ± 2716 cells per LN vs. 9063 ± 2333 cells per LN, $n = 5$ each, average ± SD). Moreover, the ratio of Kaede-red cells was higher in $CD44^{hi}$ memory T cells than in $CD44^{mid}$ naive T cells (Figure 1D). Consistently, the majority of Kaede-red migratory cells were of the $CD44^{hi}$ memory phenotype (Figure 1D). These results suggest that predominantly T cells with the memory surface phenotype migrate from the skin into DLNs, even in the steady state.

Migration of Tregs from the skin to the DLNs. Immune responses and homeostasis are regulated by the functions of memory/effector T cells and Tregs. To determine the behaviors of these populations, we intercrossed Kaede-Tg mice with Foxp3 reporter mice expressing human CD2 and human CD52 chimeric protein, which are designated as Kaede/$Foxp3^{hCD2/hCD52}$ mice. Since $Foxp3^+$ cells coexpress hCD2 on the cell surface, live $Foxp3^+$ Tregs could be labeled and sorted with anti-hCD2 monoclonal Ab. The DLN cells from Kaede/$Foxp3^{hCD2/hCD52}$ mice in the steady state were analyzed by flow cytometry. A majority of $CD25^+$ cells were hCD2 positive, but a substantial number of $hCD2^+$ cells were detected even in $CD25^-$ cells (18) (Figure 2A), which is consistent with the previous findings by the other group (19). Therefore, the following studies were performed using Kaede/$Foxp3^{hCD2/hCD52}$ mice, and $hCD2^+$ cells were considered to be Tregs.

To evaluate T cell migration from the skin in the steady state, the clipped abdominal skin of Kaede/$Foxp3^{hCD2/hCD52}$ mice was exposed to violet light as in Figure 1A, and 24 hours later, the draining axillary LN cells were subjected to flow cytometry. Con-

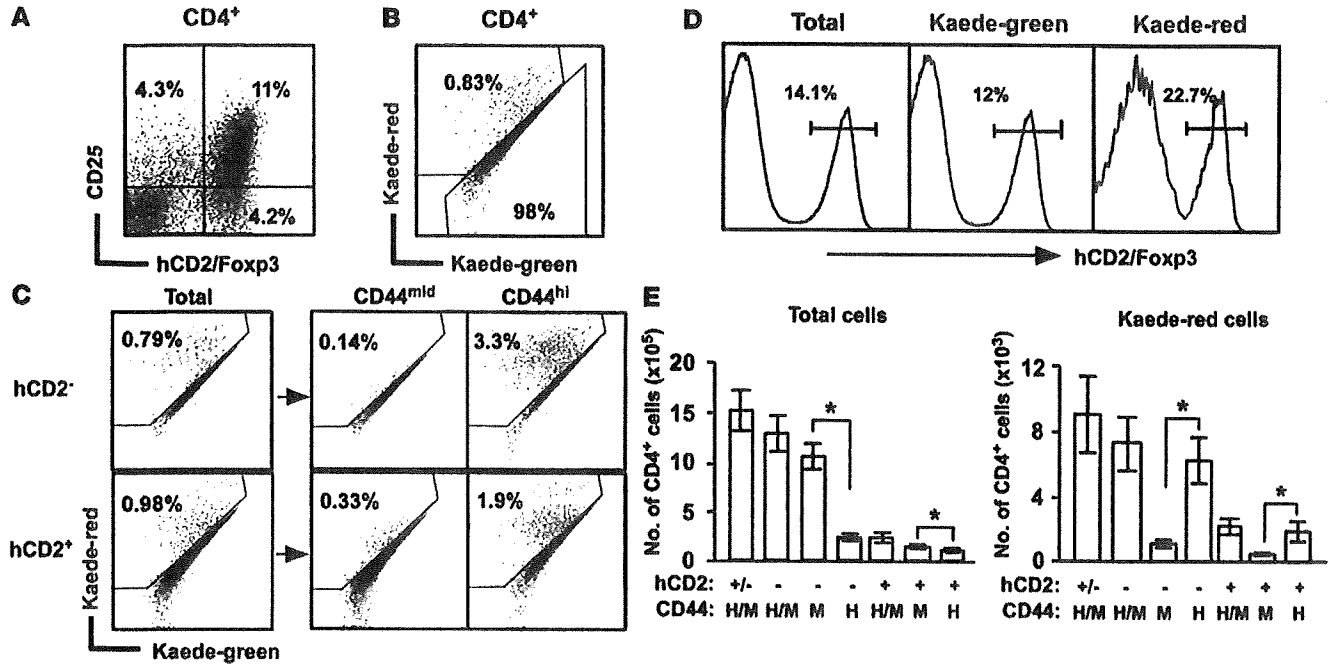

Figure 2

Migration of Tregs from the skin to DLNs. (**A**–**E**) The DLN cells of Kaede/Foxp3$^{hCD2/hCD52}$ mice photoconverted on the abdomen 24 hours prior were stained with CD4, CD25, and hCD2 mAbs. Shown here are the flow cytometric plots for hCD2/Foxp3 and CD25 staining among CD4$^+$ cells (**A**) and Kaede-red and Kaede-green expression on hCD2$^+$CD4$^+$ cells among skin DLN cells (**B**). (**C**) The DLNs and non-DLNs from the mice 24 hours after photoconversion were stained with CD4, hCD2, and CD44 mAbs and subjected to flow cytometry. (**D**) hCD2/Foxp3 expression in total (Kaede-red plus Kaede-green), Kaede-red, and Kaede-green CD4 cells was compared by flow cytometry. (**E**) The numbers of CD44^{mid} naive (M), CD44^{hi} memory (H), and naive plus memory (H/M) phenotypes of hCD2$^-$CD4$^+$ non-Tregs (–), hCD2$^+$CD4$^+$ Tregs (+), and total (hCD2$^-$ and hCD2$^+$; +/–) CD4$^+$ T cells in total CD4$^+$ (Kaede-red plus Kaede-green) cells and Kaede-red cells in the DLNs were counted. Data are presented as means ± SD and are representative of 3 independent experiments. Student's *t* test was performed between the indicated groups. $^*P < 0.05$. Numbers within plots or histograms indicate percentage of cells in the respective areas (**A**–**D**).

sistent with the previous results (Figure 1D), a substantial percentage (0.83%) of photoconverted CD4$^+$ T cells were observed in the DLNs (Figure 2B). Among hCD2$^-$ non-Tregs and hCD2$^+$ Tregs, the frequency of Kaede-red cells was comparable (0.79% vs. 0.98%) (Figure 2C), and the frequency of Kaede-red cells was higher in the CD44^{hi} memory subset than in the CD44^{mid} naive subset (Figure 2C). In addition, Kaede-red CD4$^+$ cells included a higher percentage of Tregs (22.7%) than total CD4$^+$ cells (14.1%) (Figure 2D). In total CD4$^+$ populations, the number of CD44^{hi} memory cells was lower than that of CD44^{mid} naive cells in both non-Tregs and Tregs (Figure 2E). In contrast, consistent with Figures 2C and 2D, CD44^{hi} memory cells were the major Kaede-red migrants from the skin among non-Tregs and Tregs (Figure 2E).

Treg migration from the skin during a cutaneous immune reaction. We tracked the extent of CD4$^+$ T cell migration from the skin during an immune response and sought to evaluate the role of CD4$^+$ T cells migrating from the skin. The dorsal skin of Kaede/Foxp3$^{hCD2/hCD52}$ mice was sensitized with 2,4-dinitro-1-fluorobenzene (DNFB), and 5 days later, the abdominal skin was challenged with DNFB. Two days after challenge, the abdominal skin was exposed to violet light for photoconversion, and another 24 hours later, the draining axillary LN cells were analyzed by flow cytometry (Figure 3A). The frequency of Kaede-red cells among CD4$^+$ T cells in the DLNs was increased up to 3% (Figure 3B) from that in the steady state (0.83%; Figure 2B). In addition, although 21% of total CD4$^+$ cells were Tregs, the number of hCD2$^+$ Tregs became comparable to that of non-Tregs in Kaede-red phenotype (49%; Figure 3, C and D). Again, the CD44^{hi} memory cells were major migrants from the challenged skin similarly to the steady state (Figure 3D and Figure 2E). The number of total CD4$^+$ T cells in DLN increased by 3-fold during contact hypersensitivity (CHS) compared with that in the steady state. However, the number of Kaede-red migratory non-Tregs and Tregs during CHS increased more drastically, by about 10- and 20-fold, respectively (Figure 2E and Figure 3D).

Consistent with increase of CD4$^+$ T cells migrating from the challenged skin into DLN, the numbers of both CD4$^+$ Tregs and CD4$^+$ non-Tregs were elevated when mice were sensitized and challenged compared with the steady state, and the ratio of Tregs to CD4$^+$ T cells during the immune response became higher than that in the steady state (Figure 3E). These results suggest that Tregs are more accumulated than non-Tregs in the skin during the cutaneous immune response **(4. AUTHOR: Grammar here is problematic. OK to change to "These results suggests that more Tregs than non-Tregs accumulate in the skin during the cutaneous immune response.")**.

It is known that cutaneous dendritic cells migrate into the DLNs in a CCR7-dependent manner (20) and that in humans, most circulating Tregs express skin-homing receptors and CCR7 (21). To address whether skin T cells have the potential to migrate into the regional LNs, skin cell suspensions were obtained from the ears of mice sensitized on the abdomen and challenged on the ear with DNFB and applied to a transwell assay. The Tregs showed good

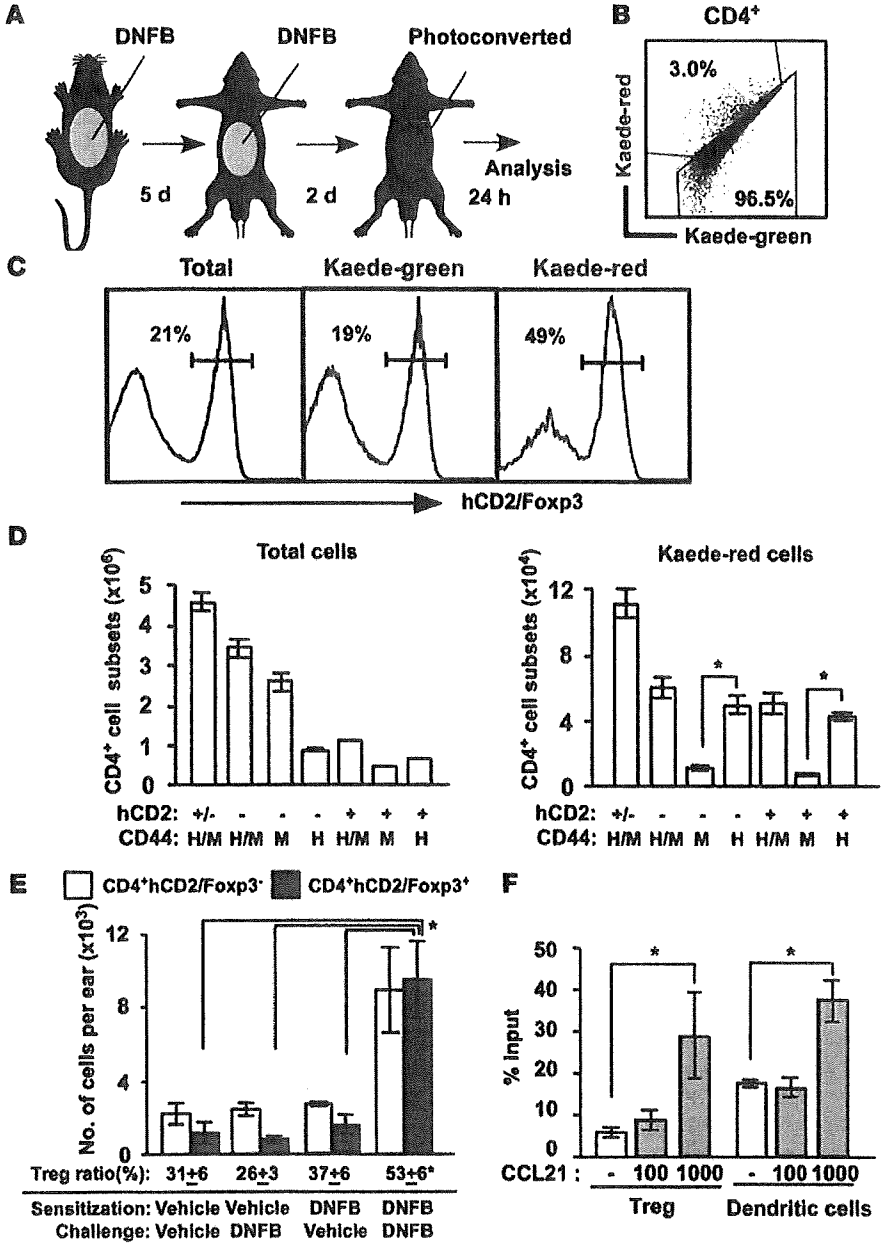

Figure 3
Cell migration from the skin to DLN during a cutaneous immune response. (**A**) Scheme of the experimental protocol is as follows: the dorsal skin of Kaede/Foxp3$^{hCD2/hCD52}$ was sensitized, and 5 days thereafter the abdominal skin was challenged. 2 days after challenge, the painted areas were photoconverted, and 24 hours after photoconversion, cells from the skin DLNs were analyzed by flow cytometry. (**B** and **C**) The frequency of Kaede-red and Kaede-green cells among CD4$^+$ cells, and the frequencies of hCD2/Foxp3+ cells in total, Kaede-green, and Kaede-red cells among CD4$^+$ cells were analyzed. Numbers within plots or histograms indicate percentage of cells in the respective areas. (**D**) The numbers of CD44^{mid} naive (M), CD44^{hi} memory (H), and naive plus memory (H/M) phenotypes of hCD2$^-$CD4$^+$ non-Tregs (–), hCD2$^+$CD4$^+$ Tregs (+), and total (hCD2$^-$ and hCD2$^+$; +/–) CD4$^+$ T cells among total CD4$^+$ cells and Kaede-red cells in the DLNs were counted. (**E**) Number of Tregs and non-Tregs in the skin. The mice were painted with DNFB or vehicle on the abdomen, followed by DNFB or vehicle application on the ears. The number of CD4$^+$ Tregs and CD4$^+$ non-Tregs and the percentage ratio of Tregs among CD4$^+$ T cells in the ears were measured. (**F**) Transwell assay. The number of hCD2$^+$CD4$^+$ cells and CD11c$^+$ cells of skin-cell suspensions from Foxp3$^{hCD2/hCD52}$ mice that migrated to the lower chamber was analyzed. Data are presented as means ± SD (**D–F**) and are representative of 3 independent experiments. Student's *t* test was performed between the indicated groups. $^*P < 0.05$ (**D–F**).

chemotactic responses to CCL21 comparable to that of MHC class II$^+$ cutaneous dendritic cells (Figure 3F). Similar chemotactic activity to CCL21 was seen in CD4$^+$ non-Tregs (data not shown). Since the ratio of Tregs and non-Tregs in Kaede-red CD4$^+$ T cells in LNs was comparable to that in the skin at the time of photoconversion, Tregs and non-Tregs in the skin seem to have equivalent propensity to migrate to the DLN. In addition, we evaluated the CCR7 expression of Tregs in the skin before and after challenge and found that Tregs in the skin expressed CCR7 both before and after challenge and that the expression level of CCR7 of Tregs after challenge was slightly lower than that before challenge (Supplemental Figure 5).

Role of Tregs in the elicitation phase of CHS. As above **(5. AUTHOR: Do you mean "As shown above"?)**, Tregs accumulate in the skin and they have the capacity to migrate to DLNs during the CHS response. These results prompted us to evaluate the role of Tregs in the cutaneous immune response. In a murine CHS model, we found that administration of Campath-1G Ab (a depleting Ab for the human CD52 antigen; ref. 22) resulted in a marked decrease in the number of Tregs in the DLNs and the skin, 1–3 days after injection (Figure 4A and data not shown) **(6. AUTHOR: Do edits to correct grammar retain your meaning?)**. Kaede/Foxp3$^{hCD2/hCD52}$ mice were sensitized with DNFB on the abdomen and treated in the presence or absence of Campath-1G Ab. The ear thickness changes after the challenge on the ears were significantly prolonged by the treatment with Campath-1G Ab at each time point compared with in control mice (Figure 4B). This enhancement of CHS response by Campath-1G Ab was not observed when C57BL/6 (B6) wild-type mice were used, which excluded the possibility of the nonspecific effect of Campath-1G Ab (Supplemental Figure 6). In addition, the ear thickness changes of mice treated with control rat IgG were

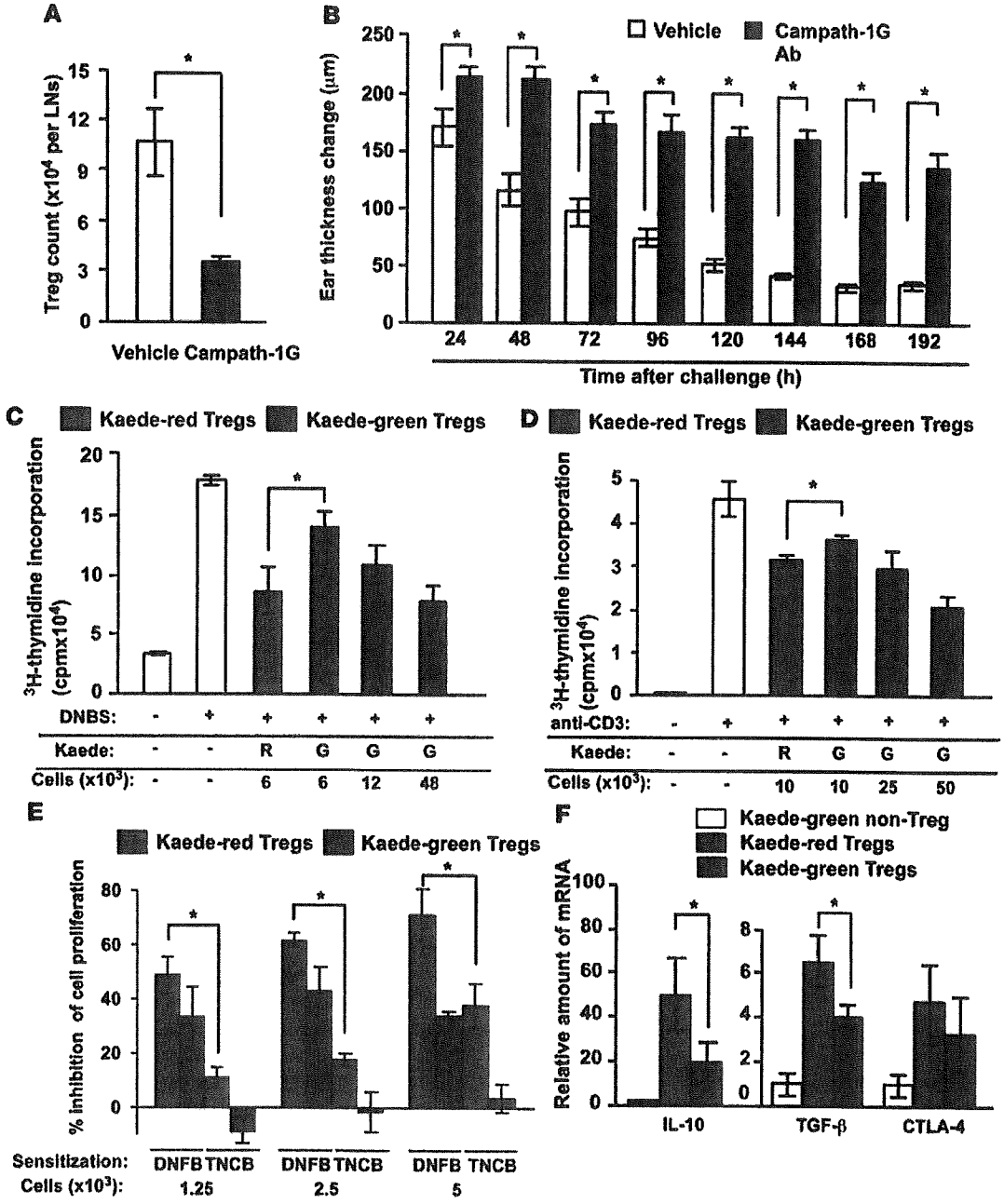

Figure 4

Enhanced ear swelling response by Treg depletion and immunosuppressive activity of Treg subsets on T cell proliferation in vitro. (**A**) The number of Tregs in the LNs after administration of Campath-1G Ab. (**B**) CHS: the Kaede/Foxp3$^{hCD2/hCD52}$ mice were sensitized, and injected with vehicle or Campath-1G Ab before challenge (n = 8 for each group). (**C**–**F**) Immunosuppressive activity of Tregs. Kaede-red and Kaede-green Tregs were sorted from the Kaede/Foxp3$^{hCD2/hCD52}$ mice, sensitized, challenged, and photoconverted. (**C**) Skin DLN cells of mice sensitized with DNFB were stimulated with DNBS in the presence or absence of Kaede-red Tregs or Kaede-green Tregs in vitro (n = 3). (**D**) Suppressive effect of Tregs in vitro. Kaede-red and Kaede-green Tregs were prepared as above and added to T cells stimulated with plate-bound anti-CD3 Ab. (**E**) Antigen specificity of Treg functions. LN cells from DNFB-sensitized or TNCB-sensitized mice were stimulated with DNBS or TNBS in vitro. Kaede-red and Kaede-green Tregs were added, and percentage inhibition of cell proliferation was evaluated as follows: (cell proliferation with DNBS or TNBS) – (cell proliferation with DNBS or TNBS in the presence of Tregs)/(cell proliferation with DNBS or TNBS) – (cell proliferation with vehicle) × 100. (**F**) Quantitative RT-PCR analysis on mRNA for *Il10* (IL-10), *Tgfb1* (TGF-β), and *Ctla4* (CTLA-4) of Kaede-red Tregs and Kaede-green Tregs. The expression of each gene was normalized by the expression of *Gapdh*, and those in Kaede-green non-Tregs were normalized to 1 (n = 3). Data are representative of 3 independent experiments and presented as means ± SD (**A**–**F**). *P < 0.05 between the indicated groups (Student's t test, **A**, **B**, **E**, and **F**; 1-way ANOVA followed by Dunnett multiple comparison test, **C** and **D**).

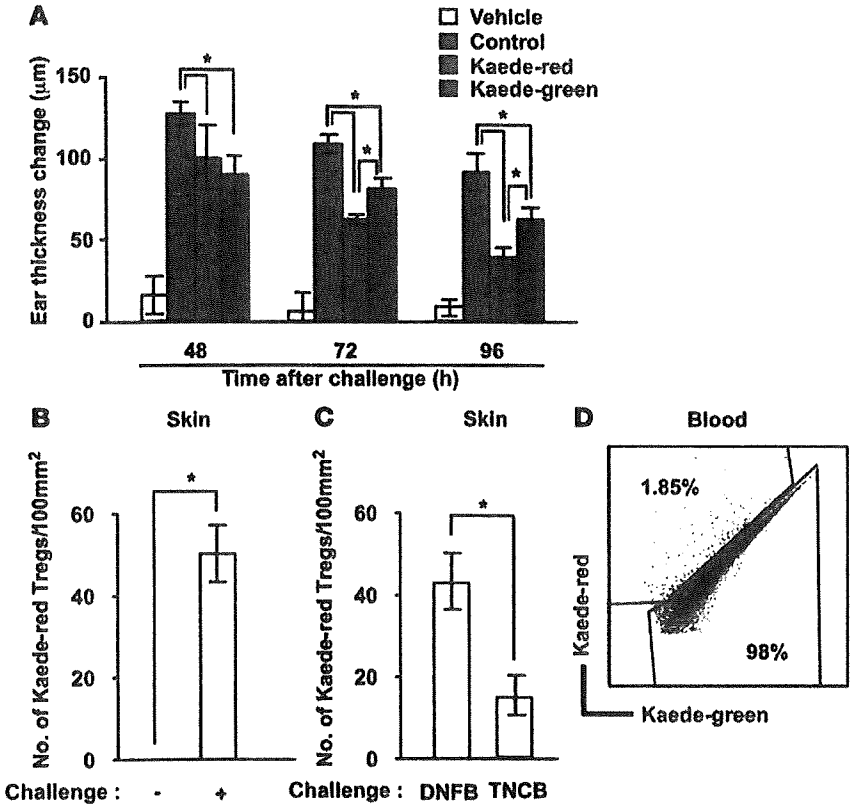

Figure 5

Immunosuppressive effect of Kaede-red Tregs in the skin. (**A**) Suppression of CHS response by Kaede-red Tregs. Kaede-red or Kaede-green Tregs (4×10^3 cells/ear) of Kaede/Foxp3$^{hCD2/hCD52}$ mice sensitized, challenged, and photoconverted as in Figure 3A were injected into ear skin of mice sensitized with DNFB 5 days prior. Immediately after injection, the mice were challenged, and the ear thickness change was measured at 48, 72, and 96 hours after challenge. (**B–D**) The mice were sensitized, challenged, and photoconverted as in Figure 3A. Twenty-four hours after photoconversion, 20 μl of 0.3% DNFB (challenge; +) or vehicle (challenge; –) (**B**) or 20 μl of 0.3% DNFB or 20 μl of 1% TNCB (**C**) was painted onto the ear. Twenty-four hours later, the ear skin and blood (**D**) were collected and dissociated for flow cytometry. The number of Kaede-red Tregs in the skin and the frequency of Kaede-red Tregs in CD4$^+$ T cell subset of the blood were evaluated ($n = 3$, each group). Data are presented as means ± SD and representative of 3 independent experiments (**A–C**). Student's t test was performed between the indicated groups. $^*P < 0.05$. Numbers within plots indicate percentage of cells in the respective areas (**D**).

comparable to those treated without Campath-1G Ab (data not shown). These results demonstrate that Tregs play an important role in the challenge phase in terminating the CHS response.

Suppressive activity of Kaede-red and Kaede-green Tregs on T cell proliferation. To further determine the suppressive function of the Tregs migrating from the skin during the cutaneous immune response, Kaede-red and Kaede-green CD4$^+$ Tregs in the skin DLN were prepared as in Figure 3A and cocultured with regional LN cells from DNFB-sensitized mice. Antigen-specific T cell proliferation induced by 2,4-dinitrobenzene sulfonic acid (DNBS), a water-soluble compound with the same antigenicity as DNFB, was significantly inhibited by addition of 6×10^3 Kaede-red Tregs (Figure 4C). On the other hand, 8 times the number of Kaede-green Tregs was required to achieve a similar magnitude of inhibitory effect of the Kaede-red Tregs (Figure 4C). These data indicate that the skin-derived Tregs have a stronger inhibitory effect on hapten-specific T cell proliferation than LN-resident Tregs. It should be noted that we might underestimate the inhibitory capacity of skin-migratory T cells relative to resident Tregs, since Kaede-green cells should have included the cells migrated from the skin before photoconversion and the cells that infiltrated to the skin after photoconversion and migrated to DLN.

We tested the effect of the Tregs on antigen-nonspecific T cell proliferation stimulated with membrane-bound anti-CD3 Ab. Kaede-red Tregs inhibited T cell proliferation more potently than did Kaede-green Tregs, and again a higher number of Tregs were required (Figure 4D) to obtain an extent of inhibition similar to that seen in Figure 4C.

To further evaluate the antigen specificity of Tregs in T cell proliferation, we isolated the DLN cells 5 days after DNFB or 2,4,6-trinitro-l-chlorobenzene (TNCB) sensitization and restimulated them with DNBS or trinitrobenzene sulfonic acid (TNBS), respectively, and added Kaede-red Tregs or Kaede-green Tregs prepared from the DLNs as in Figure 3A. Kaede-red Tregs inhibited DNBS-induced T cell proliferation more than Kaede-green Tregs (Figure 4E), as shown in Figure 4C. However, this antiproliferative effect was not seen when these Kaede-red or Kaede-green Tregs were added to TNBS-stimulated LN cells from the mice sensitized with TNCB (Figure 4E). In addition, in the criss-cross comparison, similar antigen-specificity was observed on TNCB-immunized Kaede-red Tregs (data not shown). We also analyzed mRNA expressions of inhibitory cytokines and surface molecules by quantitative RT-PCR. Kaede-red Tregs expressed higher mRNA levels of *Il10* and *Tgfb1* than Kaede-green Tregs (2, 3, 23) (Figure 4F). On the other hand, although there was no significant difference, Kaede-red Tregs tended to express higher mRNA levels of cytotoxic T lymphocyte–associated molecule-4 (*Ctla4*) than did Kaede-green Tregs (2, 3, 23) (Figure 4F). These results suggest that Tregs migrating from the skin have a more efficient suppressive potency on T cell proliferation with abundant inhibitory mediators and that this antiproliferative effect shows some antigen specificity.

Tregs recirculating from the skin inhibit local cutaneous immune response in situ. The strong ability of Kaede-red Tregs to suppress in vitro T cell proliferation prompted us to determine whether Kaede-red Tregs can inhibit a local cutaneous immune response in situ. Kaede-red or Kaede-green Tregs prepared as described (Figure 3A) were injected subcutaneously into the ears of mice sensitized with DNFB 5 days before, and the ears were elicited **(7. AUTHOR: Use of "elicited" does not make sense, and we are not sure what you mean. Please revise.)** with DNFB. The DNFB-induced ear

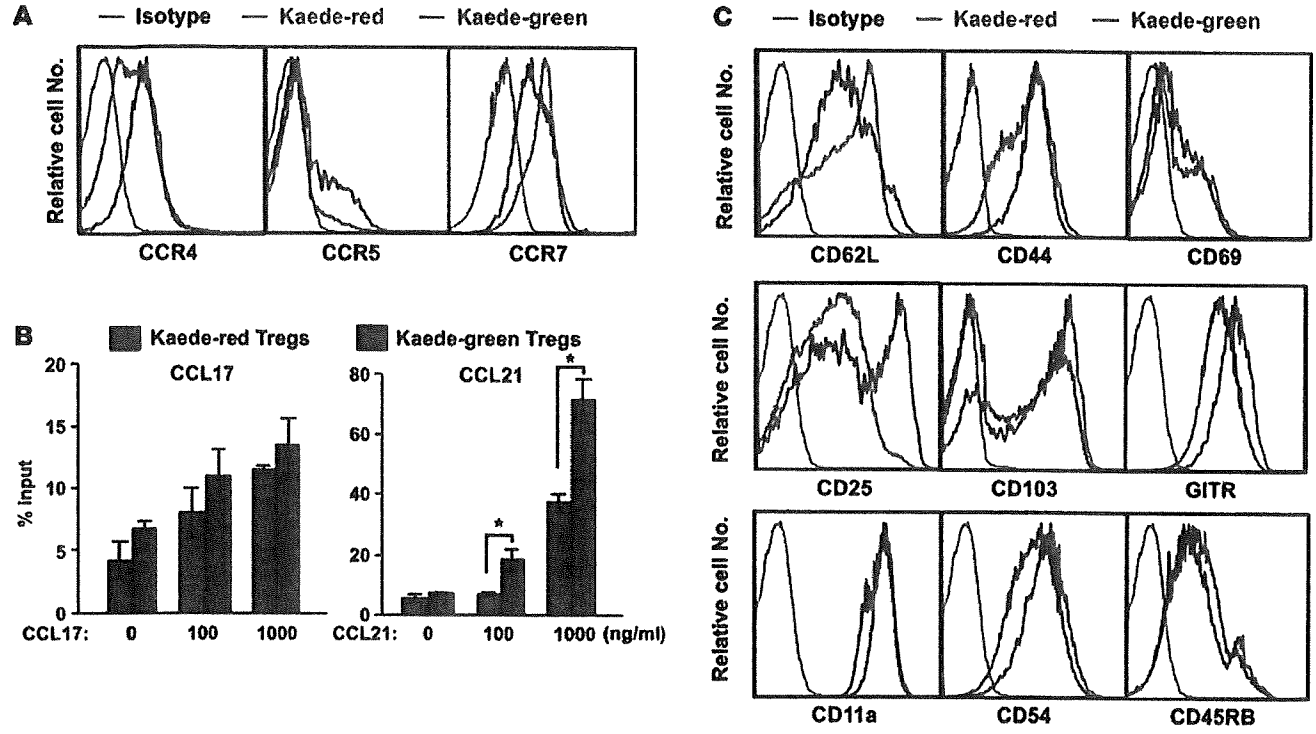

Figure 6

Surface molecule expressions on Kaede-red and Kaede-green cells. (**A**) Chemokine receptor expression. Skin DLN cells were prepared from the mice sensitized, challenged, and photoconverted as in Figure 3A. These LN cells were stained with isotype-matched control, CCR4, CCR5, and CCR7 mAbs, and the expression levels of Kaede-red and Kaede-green Tregs were evaluated by flow cytometry. (**B**) Transwell assay. DLN cells were transferred to the upper chamber of the transwell, and CCL17 or CCL21 was added to the lower chamber. The cells were incubated for 3 hours, and the numbers of Kaede-red and Kaede-green cells that migrated to lower chamber were analyzed by flow cytometry. Data are presented as means ± SD and representative of 2 independent experiments. Student's *t* test was performed between the indicated groups. $^*P < 0.05$. (**C**) Surface molecule expression. LN cells were stained with isotype-matched control, CD62L, CD44, CD69, CD25, and CD103 mAbs, and the expression levels were evaluated by flow cytometry. These data are representative of 3 independent experiments.

thickness change was suppressed by the injection of Kaede-red and Kaede-green Tregs at all time points (Figure 5A). It was noted, however, that Kaede-red Tregs suppressed CHS more than Kaede-green Tregs at 72 and 96 hours after challenge (Figure 5A).

Considering that Tregs function as a regulator for primed T cells, they should serve as suppressors at the challenged site. The above late-phase inhibitory action of Kaede-red Tregs raised the possibility that Tregs migrating from the skin can return to the skin and exert suppressive activity. Kaede/Foxp3$^{hCD2/hCD52}$ mice were sensitized, challenged, and photoconverted as in Figure 3A. Twenty-four hours after photoconversion, the left and right ears were rechallenged with DNFB and vehicle (Figure 5B) or TNCB (Figure 5C), respectively. Another 24 hours later, Kaede-red Tregs were observed in the ears challenged with DNFB, but not in those challenged with vehicle (Figure 5B). The ear rechallenged with a different hapten, TNCB, contained Kaede-red Tregs, but its number was lower than that of the ear rechallenged with DNFB (Figure 5C). In addition, Kaede-red Tregs were detected in CD4$^+$ cells of the blood 24 hours after rechallenge (1.79% ± 0.07%, average ± SEM, $n = 3$) (Figure 5D). Moreover, a previous report has suggested that LN cells migrate to the skin (24). We conducted an evaluation of this report by photoconverting DLNs. We sensitized the dorsal skin of mice with DNFB and challenged the abdominal skin with DNFB 4 days later. Two days after challenge, the DLNs of the mice were photoconverted and rechallenged on the ears with DNFB **(8. AUTHOR: OK to change to "Two days after challenge, the DLNs of the mice were photoconverted and the ears were rechallenged with DNFB"?)**. Twenty-four hours later, the ears of the skin were analyzed by flow cytometric analysis. We found that a substantial fraction of CD4$^+$ hCD2$^-$ non-Tregs and CD4$^+$ hCD2$^+$ Tregs were Kaede-red positive (Supplemental Figure 7). These results suggest that the Tregs that egressed from the skin had a capacity to remigrate to the skin upon challenge.

It has been reported that the representative chemokine receptors essential for migration of lymphocytes into the skin and LNs are CCR4 and CCR7, respectively (9, 14, 25). In addition, CCR5 may be an important chemokine receptor for Tregs to migrate into the skin (26). Kaede-red Tregs expressed higher levels of CCR4 and CCR5 and a lower level of CCR7 than Kaede-green Tregs (Figure 6A). When the skin DLN cells prepared as in Figure 3A were applied to a transwell assay, Kaede-red Tregs showed good chemotactic responses to both CCL17, a ligand for CCR4, and CCL21, a ligand for CCR7, but the chemotaxis of Kaede-red Tregs to CCL21 was weaker than that of Kaede-green Tregs (Figure 6B).

We further analyzed the surface molecules of Kaede-red Tregs in the DLNs of Kaede/Foxp3$^{hCD2/hCD52}$ mice treated as in Figure 3A. Kaede-red Tregs expressed a lower level of CD62L but higher levels of CD44 and CD69 than Kaede-green Tregs (Figure 6C), suggesting that the skin-derived Tregs show a more memory-related T cell phenotype. Interestingly, Kaede-red Tregs contained

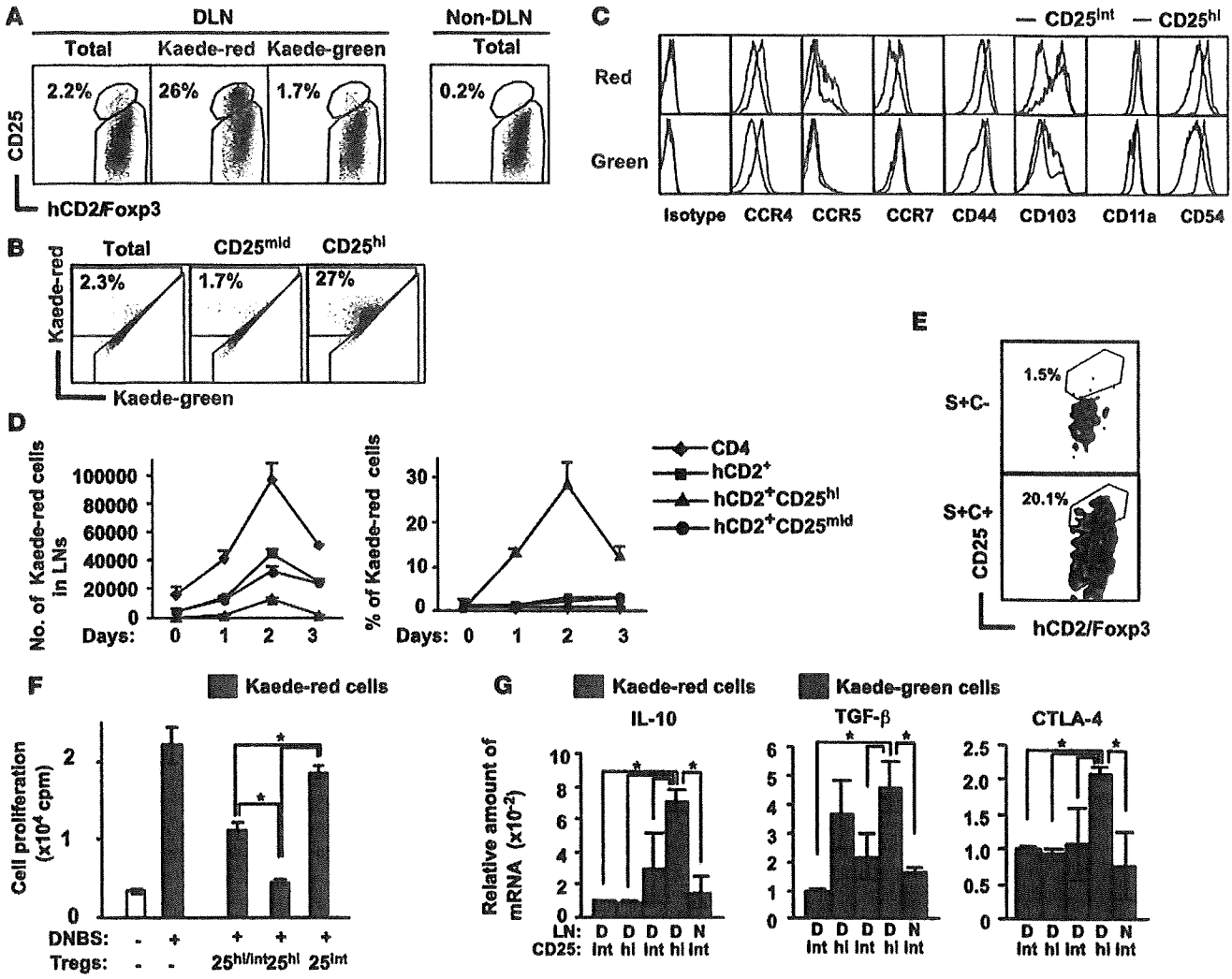

Figure 7

Kinetics and suppression activity of CD25^{hi} Kaede-red migratory Tregs. (**A–C**) Characterization of CD25^{hi} subset. Kaede/Foxp3$^{hCD2/hCD52}$ mice were treated as in Figure 3A, and the expression levels of hCD2/Foxp3 and CD25 on CD4^{+}hCD2/Foxp3^{+} Tregs in total, Kaede-red, and Kaede-green DLN cells and in non-DLN cells (**A**), the frequency of Kaede-red populations in each population (**B**), and the expression levels of surface markers on Kaede-red or Kaede-green Tregs in the DLNs (**C**) were analyzed. (**D**) Kinetics of T cell migration. Kaede/Foxp3$^{hCD2/hCD52}$ mice were sensitized and challenged as in Figure 3A and photoconverted immediately (day 0), 1 (day 1), 2 (day 2), or 3 (day 3) days after challenge. The number of each subset migrating for 24 hours after photoconversion and the frequency of Kaede-red cells among each subset were measured. (E) Foxp3$^{hCD2/hCD52}$ mice were sensitized with DNFB (S+) and challenged with DNFB (C+) or vehicle (C–). Skin suspensions were evaluated for the expression of hCD2/Foxp3 and CD25. (**F**) Skin DLNs cells of sensitized B6 mice were stimulated in the absence or presence of Kaede-red total hCD2^{+} Tregs (25$^{hi/int}$), CD25^{hi} Tregs (25^{hi}), or CD25^{int} Tregs (25^{int}). (**G**) mRNAs for *Il10* (IL-10), *Tgfb1* (TGF-β), and *Ctla4* (CTLA-4) of Kaede-green CD25^{int} or CD25^{hi} Tregs, Kaede-red CD25^{int} or CD25^{hi} Tregs, or Kaede-green CD25^{int} Tregs in DLNs (D) or non-DLNs (N) were evaluated. The expression level in Kaede-green CD25^{int} Tregs was normalized to 1. Data are presented as means ± SD (n = 3) (**D**, **F**, and **G**). *$P < 0.05$ between indicated groups. (**F** and **G**). Numbers within plots or histograms indicate percentage of cells (**A**, **B**, and **E**).

a CD25^{hi} fraction, which was barely perceptible in Kaede-green Tregs. In addition, Kaede-red Tregs expressed higher levels of CD103, an integrin important for T cell migration into the skin as well as CD11a and CD54, integrins induced upon activation, and a glucocorticoid-induced TNFR family-related gene/protein (GITR), another marker of Tregs (27, 28) (2) **(9. AUTHOR: If "2" here is a reference, please change to "(2, 27, 28)". If not, please clarify.)**. However, the expression level of CD45RB was comparable between the Kaede-red and Kaede-green Tregs. These results suggest that Kaede-red Tregs are of the memory/effector phenotype (29) and have a higher potential to migrate to the skin than LN-resident Tregs.

Kinetics and surface phenotype of CD25^{hi} Kaede-red Tregs. The above data (Figure 5A) suggest that Tregs migrating from the skin have a highly potent immunosuppressive capacity even in situ. One of the features of these skin-derived Tregs is the presence of a CD25^{hi} subset (Figure 6C) that has not, to our knowledge, been thoroughly described before. Initially, we sought to characterize the localization of CD25^{hi} Tregs and found that CD25^{hi} cells were substantially detected in Kaede-red Tregs of the DLNs of mice pretreated

as in Figure 3A but were only somewhat or marginally detected in Kaede-green Tregs of the DLNs or in non-DLNs (Figure 7A). Consistently, the frequency of the Kaede-red population in the $CD25^{hi}$ population was greater than that in the $CD25^{mid}$ population (Figure 7B). These $CD25^{hi}$ Tregs showed higher levels of CCR4, CCR5, CCR7, CD44, CD103, CD11a, and CD54 than $CD25^{int}$ Tregs in the Kaede-red subset (Figure 7C). On the other hand, the expression levels of CCR5 and CD103 of the $CD25^{hi}$ subset in the Kaede-green cells tended to be lower than that in the Kaede-red cells, and the expression of CCR7 in Kaede-green Tregs was similar between $CD25^{int}$ and $CD25^{hi}$ subsets (Figure 7C).

We then examined the kinetics of T cell migration from the skin. Kaede/$Foxp3^{hCD2/hCD52}$ mice were sensitized and challenged as in Figure 3A and photoconverted immediately, 1, 2, or 3 days after challenge. The DLN cells were collected 24 hours after each photoconversion, and the number of Kaede-red $CD4^+$, $CD4^+hCD2^+$, $CD4^+hCD2^+CD25^{hi}$, and $CD4^+hCD2^+CD25^{mid}$ cells migrating for 24 hours after photoconversion was determined (Figure 7D). The peak response of cell migration from the skin occurred on day 2 (between 48 and 72 hours after challenge) when the frequency of Tregs among $CD4^+$ T cells migrating from the skin was high (Figure 7D). In addition, $CD4^+hCD2^+CD25^{hi}$ cells were detected only at this time point (Figure 7D) and showed a high frequency of Kaede-red positivity, especially on day 2 (Figure 7D), suggesting that this subset is replaced by the skin-derived cells more readily than other subsets.

Strong immunosuppressive activity of $CD25^{hi}$ Kaede-red migratory Tregs. To evaluate whether $CD25^{hi}$ Tregs are localized in the skin during immune responses, Kaede/$Foxp3^{hCD2/hCD52}$ mice were sensitized and challenged as in Figure 3A. We detected a significant number of $CD25^{hi}$ Tregs in the challenged local skin, but few in the nonchallenged skin 48 hours after the challenge (Figure 7E), suggesting that $CD4^+hCD2^+CD25^{hi}$ cells are induced in the skin and migrate into the DLNs.

To determine the role of skin-derived $CD25^{hi}$ Tregs, Treg subsets were isolated from the DLNs of mice pretreated as in Figure 3A and cocultured with DLN cells from DNFB-sensitized mice. The $CD25^{hi}$ Tregs showed much stronger suppressive activity on T cell proliferation than the $CD25^{int}$ subset (Figure 7F).

We further examined the mRNA expression profiles of cytokines in the $CD25^{hi}$ Treg subsets. In agreement with the above in vitro result, Kaede-red $CD25^{hi}$ Tregs contained significantly higher amounts of *Il10*, *Tgfb1*, and *Ctla4* than Kaede-red $CD25^{int}$ Tregs in the DLNs, Kaede-green $CD25^{hi}$ or $CD25^{int}$ Tregs in the DLNs, or Kaede-green $CD25^{int}$ Tregs in the non-DLNs, except in the case of *Tgfb1* expression level between Kaede-red $CD25^{hi}$ Tregs and Kaede-green $CD25^{hi}$ Tregs in DLNs (Figure 7G). These results suggest that $CD25^{hi}$ Tregs migrating from the skin play a major suppressive role in cutaneous immune response.

Discussion

In this study, we found that memory/effector phenotype $Foxp3^+$ Tregs as well as $Foxp3^-$ non-Tregs migrated from the skin to DLNs in the steady state. The number of $CD4^+$ T cells in the skin and their migration to DLNs were prominently increased during a cutaneous immune response. Among the migrating T cells, $Foxp3^+$ Tregs constituted one of the major populations. Notably, the Tregs that migrated from the skin returned to the skin upon exposure to an antigen. The migrating Tregs held strong immunosuppressive effect and expressed high levels of mRNA for inhibitory mediators compared with LN-resident Tregs. Moreover, depletion of endogenous Tregs in vivo prolonged the CHS response. Finally, these circulating Tregs specifically included the $CD25^{hi}$ subset that showed an activated phenotype and a very strong inhibitory function on T cell proliferation, with high levels of mRNA for inhibitory mediators. These data suggest that Tregs circulate between blood, skin, and lymphoid tissues to regulate peripheral immune responses.

There have been a few studies that sought to address the possibility of T cell migration from the periphery to LNs. In their experiments, one report suggested that the memory/effector subset of $CD4^+$ T cells is the major constituent in the afferent lymph by cannulation of sheep (6, 11–13), and the other suggested the naive subset is dominant using subcutaneous injection of fluorescent-labeled lymphocytes (14). Recently, effector/memory phenotype of Tregs has been reported to migrate from blood to islet and to DLNs sequentially using an islet allograft model with transfer of in vitro–induced Tregs (30). However, since all the above experiments require traumatic or artificial procedures to label T cells in the periphery, it remains unknown whether endogenous T cells egress from the periphery into DLNs under pathophysiological conditions. In this study, using the Kaede-Tg system, we have clearly demonstrated that a subset of T cells with memory/effector phenotype migrates to DLNs in the steady state and during a cutaneous immune response. During the immune response, Tregs are the major constituents and they return to the skin upon exposure to an antigen. Therefore, as naive T cells circulate between blood and LNs, cells of the memory/effector T cell phenotype, especially Tregs, seem to circulate between blood and the skin **(10. AUTHOR: Do edits to correct grammar retain your meaning?)**. In this study, we used the skin as a representative of the peripheral tissues, but it would be of interest to explore this issue in other peripheral tissues, such as lungs and intestines.

To date, the roles of externally transferred Tregs in CHS have been reported (31); however, the regulatory activity of endogenous Tregs has not been fully assessed. In this study, we found that depletion of Tregs during the elicitation phase prolonged the CHS response. In addition, CHS-induced migratory Tregs suppressed the proliferation of DNFB-sensitized LN cells in a ratio as low as 1:100 (Tregs to LN cells), but such an inhibitory effect was not observed in non–antigen-specific mitogen-induced T cell proliferation systems. Therefore, Tregs circulating between the skin and LNs may inhibit not only T cells, but also antigen-presenting cells, such as dendritic cells, or antigen-presenting cell–T cell interactions. Moreover, subcutaneous injection of migratory Tregs into the skin suppressed CHS more markedly than that of LN-resident Tregs. Similar findings were observed when these Tregs were transferred intravenously (data not shown), suggesting that Tregs migrating from the skin hold a high immunosuppressive potential.

The $CD25^{hi}$ subset that migrated from the skin seems to have an activated phenotype, indicated by the positivity of CD25 and CD103. It has been reported that transfer of preactivated $CD25^+CD103^+$ cells strongly suppressed T cell proliferation (32) and $CD25^+CD103^+$ cells are the main producer of IL-10 after TCR stimulation (29). The $CD25^{hi}$ subset in our finding expresses high levels of CD103 and IL-10 and strong suppressive capacity and phenotype, consistent with an activated effector/memory Treg subset (28, 33). It should be noted that we demonstrate that the $CD25^{hi}$ subset was localized in the skin and only transiently migrated from the skin after CHS elicitation. Thus, the role of skin in generation, education, and spatiotemporal regulation of this $CD25^{hi}$ subset during immune responses needs to

be elucidated in the future, which may lead us to understand the role of peripheral tissues in regulation of immune responses.

Notably, Treg cell circulation was remarkably induced during cutaneous immune responses. Therefore, we have focused on the roles of Tregs instead of effector/memory T cells migrating from the skin. In fact, the administration of migratory Tregs strongly suppressed CHS response at the later phase after a challenge (Figure 5A), and in vivo depletion of Tregs prolonged the CHS response, particularly during the later phase (Figure 4B). These results suggest that these circulating Tregs might be involved in the termination of immune responses. However, immune responses and homeostasis are regulated and maintained by the balance between Tregs and effector/memory T cells, and it has been thought that CHS occurs by the dominance of effector/memory T cells over Tregs. Hence, it is intriguing that the elicitation of CHS induces Tregs despite their possible antagonistic role for the development of acquired immune response. In this sense, it will be of interest to explore more the roles of effector/memory T cells and Tregs migrating from the skin in regulating immune response. Clarification of these issues will lead not only to understanding of the novel mechanism of cutaneous immune responses but also to control of systemic immune responses through modulating cutaneous immunity.

Methods

Mice and photoconversion. Tg mice carrying Kaede cDNA under the CAG promoter were established previously (17). These mice with B6 genetic background expressed photoconvertible Kaede in all of their cell types. It should be noted that the use of violet light (436 nm) rather than harmful UVA (320–400 nm) or UVB (290–320 nm) allowed us to photoconvert Kaede in the cells with no detectable damage (17).

Because of the moiety of its wavelength, violet light exposure penetrates through the skin to subcutaneous tissue, but not further (data not shown). Although the exposure of Kaede to violet light permanently changes its structure and photoconverted Kaede has a very long biological half-life in lymphocytes, cell proliferation dilutes photoconverted Kaede with newly synthesized nonphotoconverted Kaede, and after several cell divisions, the detection of red fluorescence becomes difficult (17). Moreover, exposure of the cells to violet light for 10 minutes has no effect on T and B cell proliferation (17). To exclude the immunomodulatory effect of photoconversion in vivo, we used the CHS model. Photoconversion of the abdominal skin immediately after sensitization on the abdomen did not affect CHS response (data not shown). When mRNA levels of *Il1b* were examined 6 hours after photoconversion (436 nm) or low-dose (3 kJ/m^2) UVB exposure, a significant increase of mRNA levels of *Il1b* was observed by UVB but not by photoconversion (Supplemental Figure 8). Therefore, we assume that photoconversion of the skin does not provoke significant inflammation in the skin or inflammatory stimuli in keratinocytes.

B6 Foxp3$^{hCD2/hCD52}$ mice were generated by homologous recombination in a B6-derived ES cell line using a targeting construct in which cDNA encoding a human CD2 and human CD52 fusion protein along with an intraribosomal entry site was inserted into the 3′ untranslated region of the endogenous Foxp3 locus (18). All CD4$^+$Foxp3$^+$ cells expressed hCD2, but CD4$^+$ Foxp3$^-$ cells did not (data not shown), indicating that the expression of the human CD2 reporter faithfully reflects the intracellular expression of Foxp3 in Foxp3$^{hCD2/hCD52}$ mice. Foxp3$^{hCD2/hCD52}$ mice (18) were intercrossed with Kaede-Tg mice to generate Kaede/Foxp3$^{hCD2/hCD52}$ mice for further evaluation. These mice were bred in specific pathogen-free facilities at Kyoto University or RIKEN. All experimental procedures were approved by the Institutional Animal Care and Use Committee of Kyoto University Faculty of Medicine and RIKEN.

Antibodies and flow cytometry. Fluorochrome-conjugated or biotinylated anti-human CD2, anti-mouse CD4, CD11a, CD11c, CD25, CD44, CD45RB, CD62L, CD69, CD103, GITR, CCR4, CCR5, and CCR7 mAbs were obtained from BD Biosciences, eBioscience, or Biolegend. Data were acquired using the JSAN system (Bay bioscience) or FACSCanto II flow cytometry system (BD Biosciences) and analyzed with FlowJo (TreeStar).

Cell preparation from the skin and cell sorting. Briefly, the ears were removed and split into dorsal and ventral halves, and cartilage was removed. The skin of the ears was floated on 0.25% trypsin/EDTA for 30 minutes at 37°C. Then the epidermis was peeled from the dermis, and both epidermis and dermis were minced with forceps. The minced tissues were incubated for 1 hours in collagenase II (Worthington Biochemical) containing hyaluronidase and DNaseI (Sigma-Aldrich). The cell suspensions were filtered with 40 μm of cell strainer.

For cell sorting, Kaede-red Tregs or Kaede-green Tregs were purified from inguinal and axillary LNs of Kaede/Foxp3$^{hCD2/hCD52}$ mice. Briefly, the mice were sensitized and challenged with DNFB in the same way as the B6 mice for DNBS-induced cell proliferation. Two days after the challenge, cells of abdominal skin were photoconverted, and single-cell suspensions were prepared from inguinal and axillary LNs 24 hours after photoconversion. The cells of each population were sorted by the FACSAria II flow cytometry system (BD Bioscience).

Photoconversion, CHS model, in vivo Treg depletion, and cell proliferation assay. Photoconversion of the skin was performed as described previously (17). Briefly, mice were anesthetized, shaved, and exposed to violet light at 95 mW/cm^2 with a 436-nm bandpass filter using Spot UV curing equipment (SP500; USHIO).

For the CHS model, mice were immunized by application of 25 μl of 0.5% DNFB (Nacalai Tesque) in 4:1 (wt/vol) acetone/olive oil to their shaved abdomens on day 0 and challenged on the right ear on day 5 with 20 μl of 0.3% (wt/vol) DNFB (34). Ear thickness was measured before and after challenge, and ear-thickness change was calculated.

For Treg depletion in vivo, mice were injected with Campath-1G Ab through the tail vein (0.5 mg/body) 1 day before the CHS challenge (22). The injection was repeated every 4 days throughout the experiment. The same amount of vehicle or rat IgG (0.5 mg/body; Sigma-Aldrich) was used as a control.

For DNBS- or TNBS-dependent cell proliferation, mice were sensitized with 50 μl of 0.5% DNFB (wt/vol) or 50 μl of 5% TNCB (Tokyo Kasei) (wt/vol) in acetone/olive oil (4/1; vol/vol) on the dorsal skin, and 5 days later, single-cell suspensions were prepared from inguinal and axillary LNs. CD25-positive cells were depleted from the cells by Auto-MACS (Miltenyi Biotec) using PE-labeled anti-mouse CD25 antibody (eBioscience) and magnetic microbeads coated with anti-PE (Miltenyi Biotec). Less than 1% of Foxp3$^+$ cells were present in the remaining LN cells. 7×10^5 LN cells/well in a 96-well plate were cultured in RPMI 1640 containing 10% FBS with or without 50 μg/ml DNBS (Alfa Aesar) for 3 days. For TNBS stimulation, the LN cells were incubated in 2.5 mM TNBS (Tokyo Kasei) in PBS for 20 minutes at 37°C and subsequently washed 3 times in PBS, and 7×10^5 cells/well in a 96-well plate were cultured in RPMI 1640 containing 10% FBS for 3 days. Cells were pulsed with 0.5 μCi ^{3}H-thymidine for the last 24 hours of culture and subjected to liquid scintillation counting.

For the proliferation assay of anti-CD3 stimulation, spleen CD4$^+$ cells deprived of CD25$^+$ cells were sorted by auto-MACS. Then, 5×10^4 cells/well were cultured in a 96-well plate coated with 1 μg/ml of anti-CD3 antibody for 72 hours. For the last 24 hours, cells were pulsed with 0.5 μCi ^{3}H-thymidine, and its incorporation was measured.

Quantitative RT-PCR analysis. Total RNA from purified cells was isolated with the RNeasy Mini Kit (QIAGEN). Quantitative RT-PCR with the Light Cycler real-time PCR apparatus was performed according to the instructions of the manufacturer (Roche) by monitoring the synthesis of double-

stranded DNA during the various PCR cycles using SYBR Green I (Roche). For each sample, duplicate test reactions were analyzed for expression of the gene of interest, and results were normalized to those of the *Gapdh* mRNA.

In vivo immunosuppression assay. A total of 4×10^3 cells of isolated Kaede-red Tregs or Kaede-green Tregs in 20 μl PBS were subcutaneously injected into the ventral surface of each ear. Ear thickness was measured for each mouse before and at the indicated time point after elicitation with a micrometer, and the difference was expressed as ear swelling (n = 4~6 in each group).

Chemotaxis assay. Skin cell suspensions of Foxp3$^{hCD2/hCD52}$ mice were tested for transmigration across uncoated 5-μm transwell filters (Corning Costar Corp.) for 3 hours to CCL21 (R&D Systems) or medium in the lower chamber, and the numbers of cells that migrated to the lower chamber were determined by flow cytometry (35). The migration index was shown as a percentage of input by dividing with total input cells in upper chamber.

Statistics. Data were analyzed with the unpaired Student's 2-tailed t test unless otherwise stated. A P value of less than 0.05 was considered to be significant.

Acknowledgments

This study was supported in part by grants from the Ministry of Education, Culture, Sports, Science, and Technology of Japan and the Ministry of Health, Labor, and Welfare of Japan.

Received for publication August 24, 2009, and accepted in revised form December 16, 2009.

Address correspondence to: Kenji Kabashima, Department of Dermatology and Center for Innovation in Immunoregulative Technology and Therapeutics, Kyoto University, Yoshida-Konoe, Kyoto, 606-8501, Japan. Phone: 81.75.753.9502; Fax: 81.75.753.9500; E-mail: kaba@kuhp.kyoto-u.ac.jp. Or to: Michio Tomura, Laboratory for Autoimmune Regulation, Research Center for Allergy and Immunology, RIKEN, 1-7-22 Suehiro-cho, Tsurumi, Yokohama City, Kanagawa 230-0045, Japan. Phone: 81.45.503.9699; Fax: 81.45.503.9697; E-mail: tomura@rcai.riken.jp.

1. Korn T, Bettelli E, Oukka M, Kuchroo VK. IL-17 and Th17 cells. *Annu Rev Immunol.* 2009;27:485–517.
2. Sakaguchi S, Yamaguchi T, Nomura T, Ono M. Regulatory T cells and immune tolerance. *Cell.* 2008;133(5):775–787.
3. Lu LF, Rudensky A. Molecular orchestration of differentiation and function of regulatory T cells. *Genes Dev.* 2009;23(11):1270–1282.
4. Gowans JL, Knight EJ. The route of re-circulation of lymphocytes in the rat. *Proc R Soc Lond B Biol Sci.* 1964;159:257–282.
5. Gowans JL. The recirculation of lymphocytes from blood to lymph in the rat. *J Physiol.* 1959;146(1):54–69.
6. Mackay CR, Marston WL, Dudler L. Naive and memory T cells show distinct pathways of lymphocyte recirculation. *J Exp Med.* 1990;171(3):801–817.
7. Matloubian M, et al. Lymphocyte egress from thymus and peripheral lymphoid organs is dependent on S1P receptor 1. *Nature.* 2004;427(6972):355–360.
8. Campbell DJ, Debes GF, Johnston B, Wilson E, Butcher EC. Targeting T cell responses by selective chemokine receptor expression. *Semin Immunol.* 2003;15(5):277–286.
9. Campbell JJ, et al. The chemokine receptor CCR4 in vascular recognition by cutaneous but not intestinal memory T cells. *Nature.* 1999;400(6746):776–780.
10. Homey B, et al. CCL27-CCR10 interactions regulate T cell-mediated skin inflammation. *Nat Med.* 2002;8(2):157–165.
11. Olszewski WL, Grzelak I, Ziolkowska A, Engeset A. Immune cell traffic from blood through the normal human skin to lymphatics. *Clin Dermatol.* 1995;13(5):473–483.
12. Olszewski WL. The lymphatic system in body homeostasis: physiological conditions. *Lymphat Res Biol.* 2003;1(1):11–21; discussion 21–24.
13. Mackay CR, Kimpton WG, Brandon MR, Cahill RN. Lymphocyte subsets show marked differences in their distribution between blood and the afferent and efferent lymph of peripheral lymph nodes. *J Exp Med.* 1988;167(6):1755–1765.
14. Debes GF, et al. Chemokine receptor CCR7 required for T lymphocyte exit from peripheral tissues. *Nat Immunol.* 2005;6(9):889–894.
15. Ando R, Hama H, Yamamoto-Hino M, Mizuno H, Miyawaki A. An optical marker based on the UV-induced green-to-red photoconversion of a fluorescent protein. *Proc Natl Acad Sci U S A.* 2002;99(20):12651–12656.
16. Mizuno H, et al. Photo-induced peptide cleavage in the green-to-red conversion of a fluorescent protein. *Mol Cell.* 2003;12(4):1051–1058.
17. Tomura M, et al. Monitoring cellular movement in vivo with photoconvertible fluorescence protein "Kaede" transgenic mice. *Proc Natl Acad Sci U S A.* 2008;105(31):10871–10876.
18. Komatsu N, et al. Heterogeneity of natural Foxp3+ T cells: a committed regulatory T-cell lineage and an uncommitted minor population retaining plasticity. *Proc Natl Acad Sci U S A.* 2009;106(6):1903–1908.
19. Fontenot JD, Rasmussen JP, Gavin MA, Rudensky AY. A function for interleukin 2 in Foxp3-expressing regulatory T cells. *Nat Immunol.* 2005;6(11):1142–1151.
20. Randolph GJ, Ochando J, Partida-Sanchez S. Migration of dendritic cell subsets and their precursors. *Annu Rev Immunol.* 2008;26:293–316.
21. Hirahara K, et al. The majority of human peripheral blood CD4+CD25highFoxp3+ regulatory T cells bear functional skin-homing receptors. *J Immunol.* 2006;177(7):4488–4494.
22. Hale G, Cobbold SP, Waldmann H, Easter G, Matejtschuk P, Coombs RR. Isolation of low-frequency class-switch variants from rat hybrid myelomas. *J Immunol Methods.* 1987;103(1):59–67.
23. Wing K, Onishi Y, et al. CTLA-4 control over Foxp3+ regulatory T cell function. *Science.* 2008;322(5899):271–275.
24. Reiss Y, Proudfoot AE, Power CA, Campbell JJ, Butcher EC. CC chemokine receptor (CCR)4 and the CCR10 ligand cutaneous T cell-attracting chemokine (CTACK) in lymphocyte trafficking to inflamed skin. *J Exp Med.* 2001;194(10):1541–1547.
25. Randolph GJ, Ochando J, Partida SNS. Migration of dendritic cell subsets and their precursors. *Annu Rev Immunol.* 2007;26:293–316.
26. Yurchenko E, et al. CCR5-dependent homing of naturally occurring CD4+ regulatory T cells to sites of Leishmania major infection favors pathogen persistence. *J Exp Med.* 2006;203(11):2451–2460.
27. Baekkevold ES, et al. A role for CCR4 in development of mature circulating cutaneous T helper memory cell populations. *J Exp Med.* 2005;201(7):1045–1051.
28. Huehn J, et al. Developmental stage, phenotype, and migration distinguish naive- and effector/memory-like CD4+ regulatory T cells. *J Exp Med.* 2004;199(3):303–313.
29. Banz A, et al. A unique subpopulation of CD4+ regulatory T cells controls wasting disease, IL-10 secretion and T cell homeostasis. *Eur J Immunol.* 2003;33(9):2419–2428.
30. Zhang N, et al. Regulatory T cells sequentially migrate from inflamed tissues to draining lymph nodes to suppress the alloimmune response. *Immunity.* 2009;30(3):458–469.
31. Ring S, Oliver SJ, Cronstein BN, Enk AH, Mahnke K. CD4+CD25+ regulatory T cells suppress contact hypersensitivity reactions through a CD39, adenosine-dependent mechanism. *J Allergy Clin Immunol.* 2009;123(6):1287–1296 e1282.
32. Siegmund K, et al. Migration matters: regulatory T-cell compartmentalization determines suppressive activity in vivo. *Blood.* 2005;106(9):3097–3104.
33. Miyara M, et al. Functional delineation and differentiation dynamics of human CD4+ T cells expressing the FoxP3 transcription factor. *Immunity.* 2009;30(6):899–911.
34. Kabashima K, Arima Y, Miyachi Y. Contact dermatitis from lacquer in a 'Go' player. *Contact Dermatitis.* 2003;49(6):306–307.
35. Kabashima K, et al. Thromboxane A2 modulates interaction of dendritic cells and T cells and regulates acquired immunity. *Nat Immunol.* 2003;4(7):694–701.

Prostaglandin E_2–EP_3 signaling suppresses skin inflammation in murine contact hypersensitivity

Tetsuya Honda, MD, PhD,[a,b] Toshiyuki Matsuoka, MD, PhD,[a] Mayumi Ueta, MD, PhD,[c] Kenji Kabashima, MD, PhD,[b] Yoshiki Miyachi, MD, PhD,[b] and Shuh Narumiya, MD, PhD[a] *Kyoto, Japan*

Background: Prostaglandin (PG) E_2 exerts a variety of actions through 4 G protein–coupled receptors designated as EP_1, EP_2, EP_3, and EP_4. We have reported that PGE_2 acts on EP_3 in airway epithelial cells and exerts anti-inflammatory actions in ovalbumin-induced murine allergic asthma. Although EP_3 is also expressed in skin and PGE_2 is produced abundantly during skin allergic inflammation, the role of PGE_2-EP_3 signaling in skin allergic inflammation remains unknown.

Objective: We sought to investigate whether PGE_2-EP_3 signaling exerts anti-inflammatory actions in skin allergic inflammation.

Methods: We used a murine contact hypersensitivity (CHS) model and examined the role of EP_3 by using an EP_3-selective agonist, ONO-AE-248 (AE248), and EP_3-deficient mice. The inflammation was evaluated by the thickness and histology of the hapten-challenged ear. Inflammation-associated changes in gene expression and effects of AE248 were examined by means of microarray analysis of the skin. Localization of EP_3 was examined by staining for β-galactosidase knocked in at the EP_3 locus in EP_3-deficient mice. EP_3 action was also examined in cultured keratinocytes.

Results: Administration of AE248 during the elicitation phase significantly suppressed CHS compared with that seen in vehicle-treated mice. Microarray analysis revealed that administration of AE248 inhibited the gene expression of neutrophil-recruiting chemokines, including CXCL1, at the elicitation site. X-gal staining in EP_3-deficient mice revealed EP_3 expression in keratinocytes, which was further confirmed by anti-EP_3 antibody in wild-type mice. In cultured keratinocytes AE248 suppressed CXCL1 production induced by TNF-α.

Conclusion: PGE_2-EP_3 signaling inhibits keratinocytes activation and exerts anti-inflammatory actions in murine CHS. (J Allergy Clin Immunol 2009;124:809-18.)

From the Departments of [a]Pharmacology and [b]Dermatology, Kyoto University Faculty of Medicine, and [c]the Department of Ophthalmology, Kyoto Prefectural University of Medicine.

Supported in part by grants-in-aid for scientific research from the Japanese Ministry of Education, Culture, Sports, Science, and Technology; the National Institute of Biomedical Innovation of Japan; the Takeda Scientific Foundation; the ONO Research Foundation; and the Fujiwara Memorial Foundation; and Japan Society for the Promotion of Science.

Disclosure of potential conflict of interest: The authors have declared that they have no conflict of interest.

Received for publication July 22, 2008; revised April 24, 2009; accepted for publication April 24, 2009.

Available online June 22, 2009.

Reprint requests: Shuh Narumiya, MD, PhD, Department of Pharmacology, Kyoto University Faculty of Medicine, Kyoto 606-8501, Japan. E-mail: snaru@mfour.med.kyoto-u.ac.jp.

0091-6749/$36.00

doi:10.1016/j.jaci.2009.04.029

Key words: Prostaglandin E_2, EP_3 receptor, contact hypersensitivity

Murine contact hypersensitivity (CHS) is widely used as a model for contact dermatitis, a common allergic skin disorder of human subjects. The CHS model is composed of 2 phases: the sensitization phase, in which skin dendritic cells take up antigens, migrate to regional lymph nodes, and stimulate T-cell activation and differentiation, and the elicitation phase, in which effector T cells evoke immune inflammation on exposure to antigens.[1] Although the elicitation reaction is known to be mediated by IFN-γ–producing T_H1 cells and T cytotoxic type 1 cells, it is suggested that initial neutrophil infiltration is required for subsequent recruitment of T cells and development of inflammation.[2,3] On exposure to antigens in the elicitation phase, keratinocytes produce neutrophil-recruiting chemokines, such as CXCL1 and CXCL2, as well as T cell–recruiting chemokines, such as CCL17 or CCL27, which contribute to neutrophil recruitment within 12 hours after elicitation and after T-cell infiltration, respectively.[3-5] At an inflammatory site, other than chemokines or cytokines, lipid mediators, such as prostanoids, are produced abundantly, which might regulate CHS responses.[6,7]

Prostanoids, including prostaglandin (PG) D_2, PGE_2, $PGF_{2\alpha}$, PGI_2 (prostacyclin), and thromboxane A_2, are oxygenated metabolites of arachidonic acid produced by sequential catalysis of COX and respective synthases. They are produced in large amounts during inflammation in response to various stimuli and exert a variety of actions, including inflammatory swelling, pain sensation, and fever generation. Prostanoids exert these actions by acting on a family of G protein–coupled receptors, which include PGD receptor, 4 subtypes of PGE receptor (EP_1, EP_2, EP_3, and EP_4), PGF receptor, PGI receptor, and thromboxane A receptor.[8] In addition, another receptor belonging to the chemokine receptor family, CRTH2, also responds to PGD_2. PGE_2 and PGD_2 are abundantly produced in the skin during the elicitation phase of CHS.[6,9] It has been shown that PGD_2 promotes neutrophil infiltration through CRTH2 and contributes to progression of inflammation during elicitation.[9] However, the role of PGE_2 in the elicitation phase has not been fully investigated. Furthermore, if the above action of the PGD_2-CRTH2 signaling is the only PG-mediated action involved in elicitation of a CHS response, nonsteroidal anti-inflammatory drugs (NSAIDs) that inhibit COX and suppress PG production would suppress or lessen allergic inflammation in the skin. However, NSAIDs are usually without significant effects on the inflammation of CHS, suggesting the presence of other PG receptor–mediated processes that suppress inflammation.

On the basis of this hypothesis, we have examined the action of PGE_2 in allergic skin inflammation. Among EPs, we focused on

Abbreviations used
AE248: ONO-AE-248
CHS: Contact hypersensitivity
DNFB: 2,4-Dinitrofluorobenzene
HE: Hematoxylin and eosin
LT: Leukotriene
NSAID: Nonsteroidal anti-inflammatory drug
PG: Prostaglandin
PMN: Polymorphonuclear leukocyte
WT: Wild-type

EP_3 because EP_3 is expressed abundantly in the skin[10,11] and mediates suppression of allergic inflammation in the murine allergic asthma model.[12] Although EP_3 has been reported to have both proinflammatory and anti-inflammatory roles in patients with acute skin inflammation,[13,14] the role of EP_3 signaling in allergic skin inflammation has not been investigated. Here we used an EP_3-selective agonist and EP_3-deficient *(Ptger3*$^{-/-}$*)* mice and examined whether PGE_2-EP_3 signaling has anti-inflammatory action during the elicitation phase of CHS.

METHODS

Materials

Female 8- to 12-week-old C57BL/6 mice (Japan SLC, Shizuoka, Japan) and mice lacking EP_3 that were backcrossed to a C57BL/6 background for more than 10 generations[15] were used. Mice were bred at the Institute of Laboratory Animals of Kyoto University on a 12-hour light/dark cycle under specific pathogen-free conditions. All experimental procedures were approved by the Committee on Animal Research of Kyoto University Faculty of Medicine. The EP agonists ONO-DI-004 (EP_1 agonist), ONO-AE1-259 (EP_2 agonist), ONO-AE-248 (AE248; EP_3 agonist), and ONO-AE1-329 (EP_4 agonist) were kindly provided by Ono Pharmaceutical Co (Osaka, Japan). The structures, ligand-binding affinities and selectivities, and pharmacokinetic properties of each EP agonist were described.[8] 2,4-Dinitrofluorobenzene (DNFB) was purchased from Nacalai Tesque (Kyoto, Japan). Indomethacin was purchased from Sigma (St Louis, Mo).

CHS experiment

CHS was induced as previously described.[16] Briefly, mice were shaved and painted on the abdomen with 25 μL of 0.5% DNFB in acetone/olive oil (4:1). Five days later, the mice were challenged by painting with 10 μL of 0.3% DNFB on both sides of the ear. Ear thickness was measured with a thickness gage (Teclok, Nagano, Japan) before and 24 hours after the challenge, and the difference was used as a parameter of ear swelling. AE248 was diluted with saline or acetone and administered either subcutaneously in the dorsal skin or topically applied to the ear 3 times a day (30 minutes before and 3 and 8 hours after the DNFB challenge, respectively) at indicated doses. For repeated DNFB application, mice were sensitized first by means of topical application of 20 μL of 0.15% DNFB to both ears and challenged with 20 μL of 0.15% DNFB on both ears once a week for 4 weeks. Vehicle (acetone) or indomethacin (0.2 mg/mL in acetone, 20 μL per ear) was applied 30 minutes before each challenge.

Bone marrow transplantation

Bone marrow cells were taken from femurs from wild-type (WT) or *Ptger3*$^{-/-}$ donor mice and transplanted to recipient WT green fluorescent protein transgenic mice (2×10^6 cells for each mouse from the tail vein) irradiated with 8 Gy. Four weeks after transplantation, more than 97% of whole blood cells were reconstituted with donor-derived cells, which was confirmed by analyzing the expression of green fluorescent protein–positive cells among blood cells with flow cytometry, and we used those mice for experiments.

Histology

Ears were isolated 24 hours after elicitation, fixed in 10% formalin, and embedded in paraffin. Sections of 7 μm in thickness were prepared and stained with hematoxylin and eosin (HE). The number of neutrophils per a ×40 field was determined in 4 randomly chosen fields, and the average counts were determined. For EP_3 localization, X-gal staining was performed as previously described.[12] The sections were then counterstained with HE or anti-keratin 5 antibody (R&D Systems, Minneapolis, Minn). For staining of EP_3, the rabbit polyclonal antibody reactive with murine EP_3 (Cayman, Ann Arbor, Mich) was used as previously described.[17]

Real-time RT-PCR

Total RNA was obtained from keratinocytes of murine ear skin by using the RNeasy Mini Kit (Qiagen, Hilden, Germany). Complementary DNA was synthesized with Superscript III (Invitrogen, Carlsbad, Calif). The amount of mRNA for CXCL1 and glyceraldehyde-3-phosphate dehydrogenase was quantified by means of real-time RT-PCR with the LightCycler 2.0 (Roche Diagnostic, Foster City, Calif). The primer sequences of glyceraldehyde-3-phosphate dehydrogenase were previously described.[18] Primers used for CXCL1 were 5′-GCC TAT CGC CAA TGA GC-3′ (forward) and 5′-TGG ACA ATT TTC TGA ACC AAG-3′ (reverse). Data were analyzed by using LightCycler Software Version 4.0.

Keratinocyte culture and ELISA

Normal human epidermal keratinocytes were obtained from Kurabo (Okayama, Japan) and cultured in Humedia KG2 medium (Kurabo). Cells in the third passage were seeded in triplicate at 5×10^4 cells/well onto 24-well plates in 0.5 mL of Humedia KB2 and cultured for 24 hours. The cells were washed, incubated with 10 μmol/L AE248 for 15 minutes, and then incubated with 10 ng/mL TNF-α in the continued presence of AE248 in Humedia KB2 containing 1 μmol/L indomethacin for 6 hours. The supernatant was collected, and the amount of CXCL1 was determined by means of ELISA (R&D Systems).

DNA microarray analysis

Total RNA was prepared from DNFB-challenged ears by using TRIzol reagent (Invitrogen) and purified by using the RNeasy Mini Kit (Qiagen), and 3.5 μg of purified RNA was used for microarray analysis with a Mouse Genome 430 2.0 Array (Affymetrix, Santa Clara, Calif), according to the manufacturer's protocol. Data were analyzed by using Statistical Algorithm with the Affymetrix GeneChip Expression Analysis software (Microarray Suite 5.0). All microarray data are deposited in Gene Expression Omnibus (GEO).

Statistics

Data were expressed as means ± SEMs, and statistical analyses were performed by means of ANOVA or the Student *t* test, as appropriate. A P value of less than .05 was considered statistically significant.

RESULTS

Effect of EP_3 agonist on the elicitation phase of CHS

We first examined whether stimulation of EP_3 had an anti-inflammatory effect on CHS. To investigate this, we administered an EP_3 agonist CAE248, 100 μg/kg subcutaneously 3 times a day during the elicitation phase. This dose of AE248 exerts a significant effect *in vivo*.[12] The DNFB challenge caused ear swelling in both vehicle-treated and AE248-treated mice. However, the mice treated with AE248 showed significant reductions in swelling

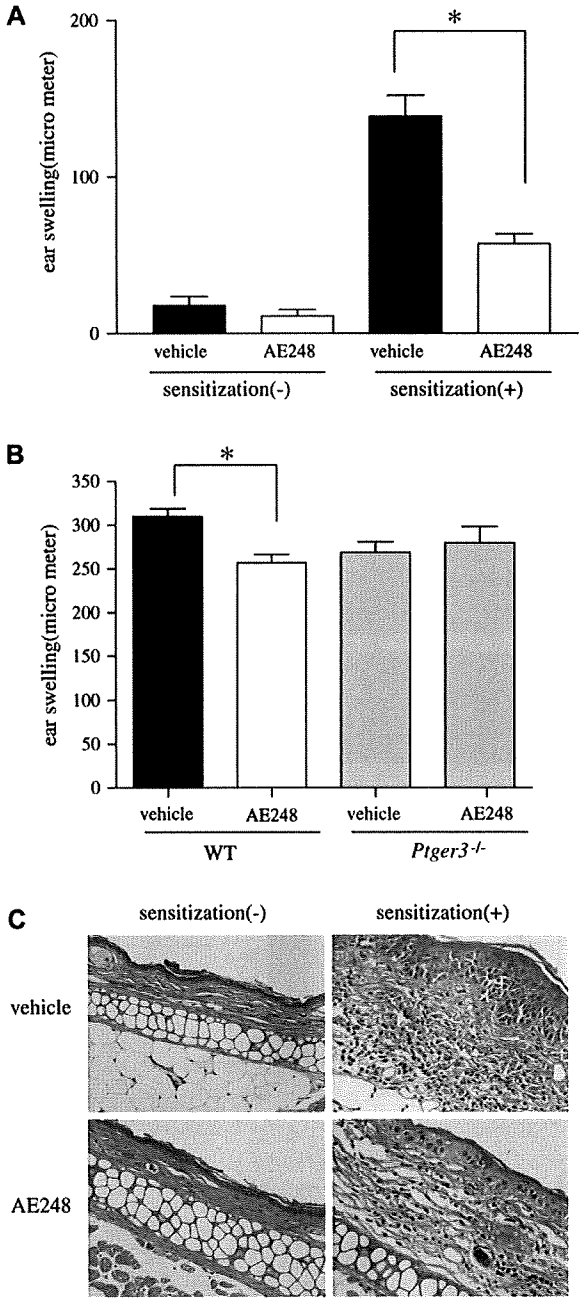

FIG 1. Suppressive effects of EP_3 agonist on the ear-swelling response in mice with CHS. **A** and **B**, Results are expressed as means ± SEMs (n = 5 in both groups). Data are representative of 3 experiments. **C**, HE staining of control- and DNFB-challenged ears treated with either vehicle or EP_3 agonist. Representative samples of each group are shown.

compared with that seen in the vehicle-treated mice 24 hours after elicitation (Fig 1, *A*). This suppressive effect of AE248 was completely absent in *Ptger3*$^{-/-}$ mice (Fig 1, *B*), suggesting that the effect was elicited through the EP_3 receptor. Histology of the ear from sensitized mice showed edema and marked inflammatory cell infiltration in the dermis 24 hours after elicitation (Fig 1, *C*). Consistently, the extent of the edema and inflammatory cell infiltration was markedly reduced in the AE248-treated mice compared with that seen in the vehicle-treated mice. These findings together demonstrate that EP_3 stimulation in the elicitation phase elicits suppressive effect on CHS.

We next examined the localization of EP_3 in the normal murine ear. X-gal staining was performed in *Ptger3*$^{-/-}$ mice, in which the β-galactosidase gene was knocked in at the EP_3 gene locus. Positive signals were detected mostly in the basal layer of epidermis in the skin of control mice (Fig 2, *A*). Similar signals were also observed in the ears of mice after elicitation, whereas little signals were detected in the cells infiltrating the dermis (data not shown). These findings suggest that the main cell species expressing EP_3 in the skin is keratinocytes and that they express it constitutively. To examine the EP_3 expression in keratinocytes of the basal layer, we costained for keratin 5, a specific marker of basal keratinocytes, and found that signals for keratin 5 colocalized with those of the X-gal staining (Fig 2, *A*). EP_3 expression in keratinocytes was confirmed by means of immunohistochemical analysis with anti-EP_3 antibody in WT mice (Fig 2, *B*). These results, together with our finding that little X-gal staining was detected in lymph nodes (data not shown), suggest a possibility that AE248 acts on keratinocytes and not on immune cells to exert its anti-inflammatory actions. Therefore we next examined the effects of topical application of AE248 to the ear in CHS. AE248 was dissolved in acetone and topically applied to the ear 3 times in the elicitation phase. This topical application of AE248 showed significant dose-dependent suppression of ear swelling in CHS 24 hours after elicitation (Fig 2, *C*), whereas that of agonists specific to other EP subtypes was without effect (Fig 2, *D*). Administration of AE248 showed a suppressive effect 24, 48, and 72 hours after elicitation, suggesting that the effect of AE248 did not induce just the delay in the development of inflammation (Fig 2, *E*). To confirm that the effect of AE248 was not caused by immune cells, we made bone marrow chimera in which stromal cells, such as keratinocytes, express EP_3, whereas bone marrow–derived cells do not express EP_3, as described in the Methods section. A suppressive effect of AE248 on ear swelling in CHS of the bone marrow chimera was detected (Fig 2, *F*), which supports our hypothesis that AE248 acts on EP_3 in keratinocytes to exert an anti-inflammatory effect.

Reduced expression of genes related to inflammatory cell infiltration caused by topical treatment with AE248

Various inflammation-related genes, including those for chemokines, are upregulated during the elicitation phase of CHS.[5] We therefore compared gene expression between vehicle-treated control mice and mice treated with AE248 to examine the role of EP_3 in this process. We first examined the time course of gene expression during the elicitation phase in our model. Ears challenged with DNFB were isolated at 1, 3, 6, 12, and 24 hours after elicitation for microarray analysis by using an Affymetrix Mouse Genome 430 2.0 GeneChip that contains 45,101 genes. We screened for gene expression, which exhibited a more than 2-fold increase at any given time during the elicitation phase over basal expression at 0 hours (Table I). Among the genes with increased expression, we focused on chemokine genes. At 1 hour after challenge, 130 genes were detected as genes showing a more than 2-fold increase in expression, and none of chemokine genes was among those genes. At 3 hours, 263 genes were upregulated, and 4 kinds of chemokines were included in this group. The analysis similarly picked up 408 genes with 5 kinds of chemokine genes at 6 hours, 655 genes with 8 kinds of chemokine genes at 12 hours, and 902 genes with 14 kinds of chemokine

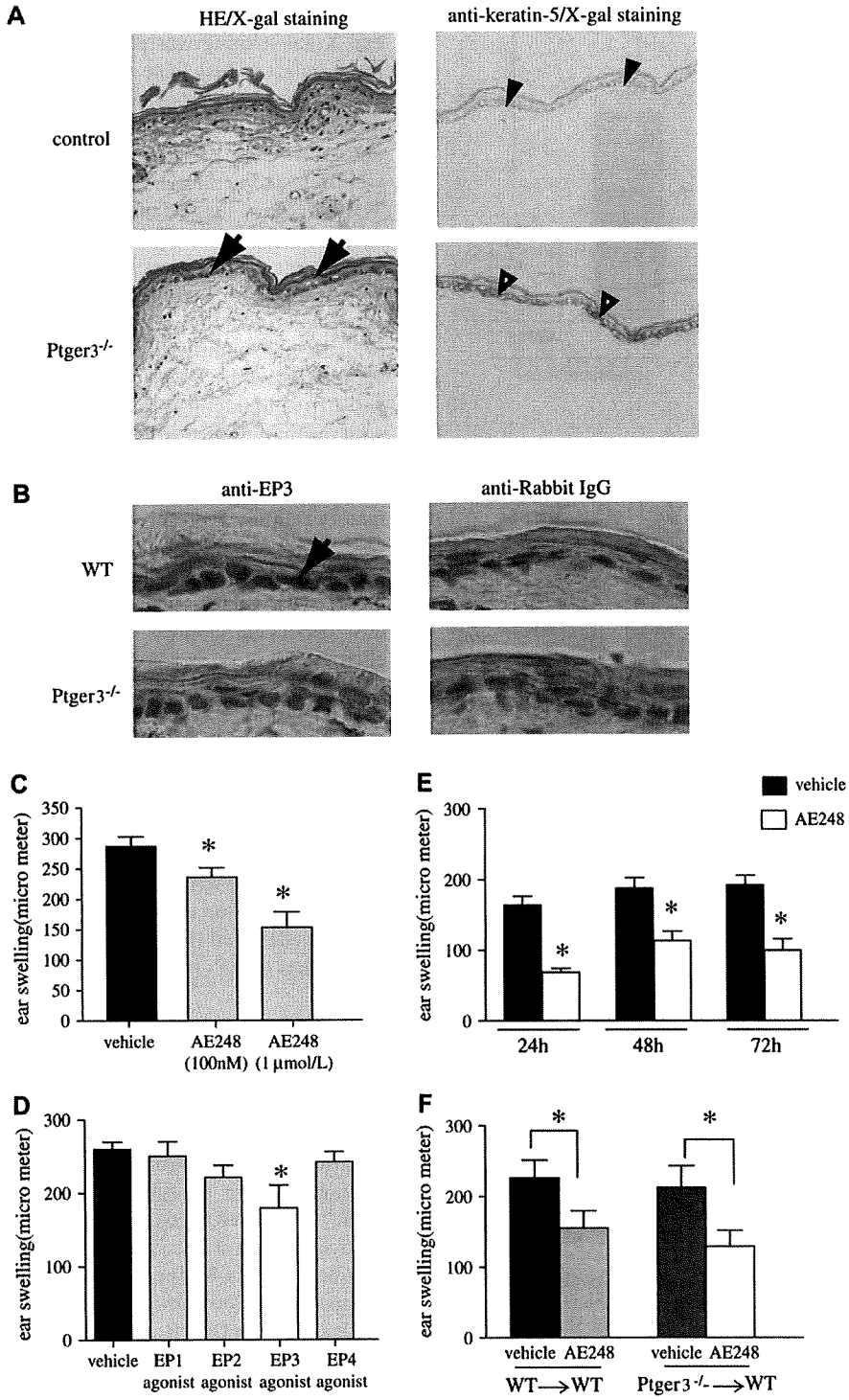

FIG 2. Localization of EP_3 receptors and effect of topical application of EP_3 agonist on mice with CHS. **A,** Histochemical staining for EP_3 (X-gal) counterstained with HE or anti-keratin 5 antibody. *Arrows,* Positive signaling (blue); *black arrowheads,* positive staining of keratin 5; *white arrowheads,* colocalization of positive signals in X-gal and anti-keratin 5 staining. **B,** Immunohistologic analysis for EP_3. The *arrow* indicates positive signals. **C-E,** Suppressive effects of topical administration of EP_3 agonist and effects of various EP agonists (1 μmol/L) on murine CHS (n = 5 per group [Fig 2, *C*] and n = 4 per group [Fig 2, *D* and *E*]). Data are representative of 2 experiments. **F,** Effect of AE248 on murine CHS of bone marrow chimera (n = 13-15 per group). Results are a combination of 3 independent experiments.

TABLE I. Time course of chemokine-related genes with expressions upregulated more than 2-fold in the elicitation phase

Time (h)	No. of genes	Gene title	Gene symbol	Probe set ID	Change ratio
1	130				
3	263	Chemokine (C-X-C motif) ligand 1	*Cxcl1*	1419209_at	2.2
		Chemokine (C-X-C motif) ligand 1	*Cxcl1*	1441855_x_at	1
		Chemokine (C-X-C motif) ligand 2	*Cxcl2*	1449984_at	1.3
		Chemokine (C-C motif) ligand 7	*Ccl7*	1421228_at	1.3
		Chemokine (C-C motif) ligand 20	*Ccl20*	1422029_at	1.2
6	408	Chemokine (C-C motif) ligand 17	*Ccl17*	1419413_at	2.6
		Chemokine (C-C motif) ligand 20	*Ccl20*	1422029_at	2.6
		Chemokine (C-X-C motif) ligand 1	*Cxcl1*	1419209_at	2.5
		Chemokine (C-X-C motif) ligand 1	*Cxcl1*	1457644_s_at	1
		Chemokine (C-X-C motif) ligand 16	*Cxcl16*	1449195_s_at	1.2
		Chemokine (C-C motif) ligand 9	*Ccl9*	1417936_at	1
12	655	Chemokine (C-X-C motif) ligand 9	*Cxcl9*	1456907_at	4.5
		Chemokine (C-X-C motif) ligand 9	*Cxcl9*	1418652_at	2.9
		Chemokine (C-X-C motif) ligand 1	*Cxcl1*	1419209_at	3.8
		Chemokine (C-X-C motif) ligand 1	*Cxcl1*	1441855_x_at	2.2
		Chemokine (C-X-C motif) ligand 1	*Cxcl1*	1457644_s_at	2.1
		Chemokine (C-X-C motif) ligand 16	*Cxcl16*	1449195_s_at	1.4
		Chemokine (C-C motif) ligand 9	*Ccl9*	1417936_at	1.2
		Chemokine (C-X-C motif) ligand 10	*Cxcl10*	1418930_at	2.8
		Chemokine (C-C motif) ligand 20	*Ccl20*	1422029_at	2.4
		Chemokine (C-X-C motif) ligand 2	*Cxcl2*	1449984_at	1.7
		Chemokine (C-C motif) ligand 2	*Ccl2*	1420380_at	1.2
24	902	Chemokine (C-X-C motif) ligand 9	*Cxcl9*	1418652_at	5.2
		Chemokine (C-X-C motif) ligand 9	*Cxcl9*	1456907_at	5.1
		Chemokine (C-X-C motif) ligand 10	*Cxcl10*	1418930_at	4
		Chemokine (C-C motif) ligand 17	*Ccl17*	1419413_at	2.5
		Chemokine (C-C motif) receptor 1	*Ccr1*	1419609_at	2.4
		Chemokine (C-X-C motif) ligand 1	*Cxcl1*	1419209_at	2.2
		Chemokine (C-C motif) ligand 12	*Ccl12*	1419282_at	2.1
		Chemokine (C-C motif) ligand 2	*Ccl2*	1420380_at	2
		Chemokine (C-X-C motif) ligand 2	*Cxcl2*	1449984_at	1.8
		Chemokine (C-C motif) ligand 9	*Ccl9*	1448898_at	1.4
		Chemokine (C-C motif) ligand 9	*Ccl9*	1417936_at	1.2
		Chemokine (C-C motif) receptor 2	*Ccr2*	1421186_at	1.3
		Chemokine (C-C motif) ligand 7	*Ccl7*	1421228_at	1.3
		Chemokine (C-C motif) ligand 19	*Ccl19*	1449277_at	1.3
		Chemokine (C-X-C motif) ligand 16	*Cxcl16*	1449195_s_at	1.2
		Chemokine (C-C motif) ligand 8	*Ccl8*	1419684_at	1

genes at 24 hours. Because these results show the most prominent change in gene expression at 24 hours after elicitation, we chose this time and compared gene expression in the ears of vehicle-treated mice with that in ears of AE248-treated mice (Fig 3). Among the 902 genes, the signal intensity of 178 genes was significantly decreased in the AE248-treated group compared with that seen in the vehicle-treated group (cluster A), and signal intensity of 183 genes was significantly increased in the AE248-treated group (cluster B). The signal intensity of the other 541 genes was not significantly different between the groups. As for chemokine genes of significant signal intensity, cluster A includes genes for 3 chemokines: CXCL1, CXCL9, and CXCL16. Among them, expression of CXCL1 was most strongly suppressed by the AE248 treatment; the signal intensity decreased to 52% compared with the control intensity (Table II), and the average intensity of the other 2 chemokine genes, CXCL9 and CXCL16, decreased to 62% and 69%, respectively, compared with the control intensity. On the other hand, 4 chemokine genes, CCL19, CCL9, CCL8, and CCL12, were detected in cluster B. The average signal intensity of CCL19, CCL9, CCL8, and CCL12 in the AE248-treated group was 129%, 268%, 368%, and 404%, respectively, of that in the vehicle-treated group. Thus the treatment with AE248 did not decrease all of the chemokines upregulated 24 hours after the challenge. However, it nonetheless suppressed the inflammatory response in CHS, indicating that suppression of the expression of the chemokine genes in cluster A (ie, CXCL1, CXCL9, and CXCL16) has an important role in the CHS response. CXCL1 binds to CXCR2 and is one of the strong neutrophil-attracting chemokines. CXCL9 recruits T_H1 cells by binding cell-surface CXCR3 and contributes to the development of CHS.[5] CXCL16 is known to bind and activate the chemokine receptor CXCR6, which is expressed on T cells and natural killer T cells.[19] Given the critical role of CXCL1 and neutrophils in the development of CHS,[2,3] we further examined the roles of CXCL1 and neutrophils in CHS. We performed real-time RT-PCR analysis and confirmed that the expression of CXCL1 mRNA was

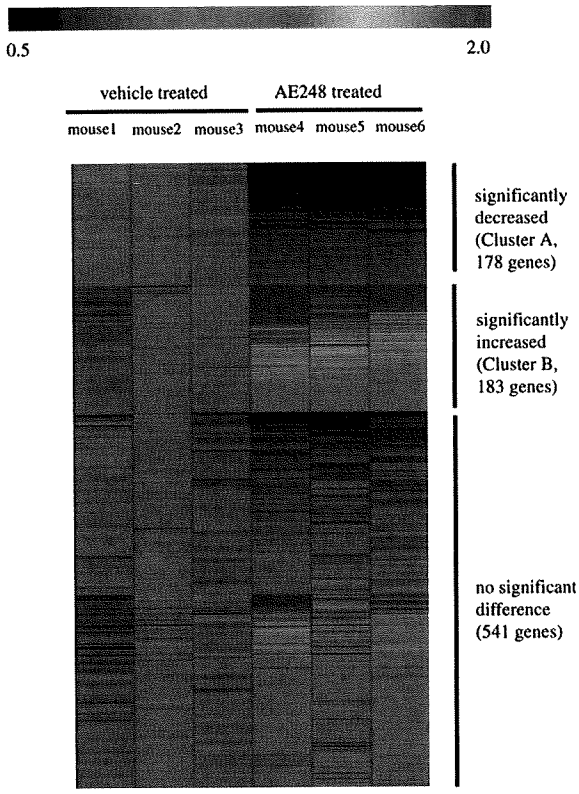

FIG 3. Microarray analysis for the effect of AE248 on gene expressions. Genes with a signal intensity that increased more than 2-fold in 24 hours at elicitation from baseline are selected (total of 902 genes). The signal intensity of each gene in the AE248-treated group (n = 3) was compared with the average signal intensity of each gene in the vehicle-treated group (n = 3), and the change ratio was indicated by means of color gradation.

significantly decreased in the AE248-treated group compared with that seen in the vehicle-treated group (data not shown). CXCL1 is produced mainly by keratinocytes in the elicitation phase of CHS. To confirm whether differences in gene expression result from differences in cell composition rather than from changes in gene expression in keratinocytes, we next examined the effect of AE248 on the mRNA expression of CXCL1 in keratinocytes from murine ear skin. We purified keratinocytes as shown in the Methods section of this article's Online Repository at www.jacionline.org. We then examined CXCL1 mRNA expression in purified keratinocytes and found that the AE248-treated group had significantly lower CXCL1 mRNA expression compared with that seen in the vehicle-treated group (Fig 4, *A*). We further examined the effect of AE248 on the production of CXCL1 by cultured keratinocytes *in vitro*. We found that keratinocytes activated with TNF-α produced a significant amount of CXCL1, and the administration of AE248 significantly suppressed the CXCL1 production (Fig 4, *B*). We next compared neutrophil (polymorphonuclear leukocytes [PMNs]) infiltration in the ears of the vehicle-treated and AE248-treated mice, as shown in the Methods section. We detected a number of PMNs in the dermis of the ear 24 hours after elicitation, whereas only a few cells were detected in the dermis of control animals. We also detected PMNs in the ears of the AE248-treated mice. However, the number of PMNs was significantly reduced in the AE248-treated mice compared with that seen in the vehicle-treated group (Fig 4, *C*). Because the average signal intensity of CXCL2 in microarray analysis, which is another important chemokine for neutrophil recruitment, was 44% of the vehicle-treated group in the AE248-treated group, we examined the CXCL2 mRNA expression in purified keratinocytes. We found that the AE248-treated group had significantly lower CXCL2 mRNA expression compared with that seen in the vehicle-treated group (see Fig E1 in this article's Online Repository at www.jacionline.org). These results combined together suggest a possibility that EP_3 exerts its anti-inflammatory effect by acting directly on keratinocytes and inhibiting neutrophil infiltration through downregulation of neutrophil-recruiting chemokines.

Involvement of endogenous PGE_2-EP_3 signaling in the development of CHS

We next examined the involvement of endogenous PG signaling in the development of CHS by applying indomethacin topically to the elicitation site. Because the effects of indomethacin were hard to detect in the usual CHS protocol (data not shown), we adopted the repetitive challenge model of CHS (repeated-challenge CHS) and examined the effect of indomethacin on the model as in the Methods section. Mice treated with indomethacin showed significantly increased ear swelling compared with the vehicle-treated mice (Fig 5, *A*), suggesting that endogenous PG produced locally in the challenged skin plays a suppressive role in inflammation of repeated-challenge CHS. We next examined the involvement of PGE_2-EP_3 signaling in this process by subjecting *Ptger3*$^{-/-}$ mice to repeated-challenge CHS. Similarly to the indomethacin-treated mice, *Ptger3*$^{-/-}$ mice exhibited significantly increased ear swelling compared with that of WT mice, and this enhancement continued 72 hours after elicitation (Fig 5, *B*). HE staining showed increased inflammatory cell infiltration in *Ptger3*$^{-/-}$ mice compared with that seen in WT mice (Fig 5, *C*). These results suggest that PGE_2-EP_3 signaling functions endogenously to negatively modulate the development of repeated-challenge CHS.

DISCUSSION

In the present study we have made the following findings. First, systemic administration of AE248, an EP_3 agonist, during the elicitation phase, can suppress inflammation in mice with CHS. Data of X-gal staining and immunohistochemical analysis demonstrated predominant EP_3 expression in keratinocytes, and topical application of AE248 to the ear skin resulted in suppression of CHS. Microarray analyses revealed that administration of AE248 modulates CHS-induced gene expression in the lesional skin either way; a decrease and an increase were demonstrated in clusters A and B, respectively. Among the chemokine genes regulated by AE248, CXCL1 was the most strongly suppressed. Consistently, AE248 suppressed CXCL1 production by TNF-α–activated keratinocytes *in vitro*. Finally, local treatment with indomethacin or the loss of EP_3 exacerbated inflammatory response to the repeated-challenge CHS. These results suggest that endogenous PGE_2 acts on EP_3 in keratinocytes *in situ* in the skin to modulate the extent of inflammation of CHS and that stimulation of PGE_2-EP_3 signaling with exogenously added agonist can control allergic inflammation in the skin.

The importance of keratinocytes in inflammatory skin diseases, such as contact dermatitis,[2,4] atopic dermatitis,[20] and psoriasis,[21,22]

TABLE II. Top 20 genes with signal intensities that were significantly decreased in AE248-treated mice compared with those in vehicle-treated mice

Gene title	Gene symbol	Probe set ID	Signal intensity		Percentage of AE248/vehicle
			Vehicle	AE248	
Solute carrier family 26, member 4	*Slc26a4*	1419725_at	2431	664.6	27.3
Matrix metallopeptidase 10	*Mmp10*	1420450_at	3371	1152	34.2
PG-endoperoxide Synthase 2	*Ptgs2*	1417262_at	3377	1345	39.8
SH2 domain containing 5	*Sh2d5*	1436100_at	2729	1118	41
Small proline-rich protein 2I	*Sprr2i*	1422963_at	13751	6136	44.6
Serine (or cysteine) peptidase inhibitor, clade E, member 1	*Serpine1*	1419149_at	801.6	359	44.8
Interferon-activated gene 202B	*Ifi202b*	1457666_s_at	15766	7122	45.1
Solute carrier family 29 (nucleoside transporters), member 2	*Slc29a2*	1447748_x_at	359.4	166.6	46.4
Fos-like antigen 1	*Fosl1*	1417487_at	3827	1785	46.6
IL-6	*Il6*	1450297_at	2010	955.7	47.6
Heparin-binding EGF-like growth factor	*Hbegf*	1418349_at	3090	1490	48.2
Cardiotrophin-like cytokine factor 1	*Clcf1*	1437270_a_at	1047	530.9	50.7
Chemokine (C-X-C motif) ligand 1	*Cxcl1*	1419209_at	4085	2131	52.2
Nucleolar complex–associated 2 homolog *(S cerevisiae)*	*Noc2l*	1424323_at	1638	867.1	52.9
RIKEN cDNA 2310002A05 gene /// hypothetical protein LOC630971	*2310002A05Rik /// LOC630971*	1456248_at	25273	13462	53.3
Similar to late cornified envelope protein	*LOC545548*	1456001_at	19223	10243	53.3
Sulfiredoxin 1 homolog *(S cerevisiae)*	*Srxn1*	1426875_s_at	4664	2525	54.1
Defensin β 3	*Defb3*	1421806_at	17218	9328	54.2
Serine (or cysteine) peptidase inhibitor, clade A (α-1 antiproteinase, antitrypsin), member 9	*Serpina9*	1429285_at	1362	750.5	55.1
RIKEN cDNA 2310007F04 gene	*2310007F04Rik*	1429641_x_at	9952	5505	55.3

The average signal intensity of each gene was compared between vehicle-treated mice and AE248-treated mice.
EGF, Epidermal growth factor.

has now received much attention. In CHS keratinocytes produce various chemokines and regulate inflammatory cell infiltration. For example, it was previously shown that blockade of CCL27, which is produced from keratinocytes and attracts memory T cells to the skin, reduced T-cell infiltration and led to the suppression of CHS,[4] and inhibition of CCL8 produced from keratinocytes suppressed CHS.[22] In this study we found that EP_3 is expressed in keratinocytes and that administration of EP_3 agonist suppresses CXCL1 mRNA expression and its production in keratinocytes. CXCL1 is a strong attractant of neutrophils and is produced mainly by keratinocytes in the elicitation phase of CHS.[2,3] Recently, it has been reported that infiltration of neutrophils is required for the development of inflammation in CHS.[2] Depletion of neutrophils in hapten-challenged mice decreased the number of IFN-γ–producing T cells at elicitation sites, which resulted in the inhibition of CHS response, and injection of neutrophils into ears restored the CHS response.[2,3] Administration of anti-CXCL1 serum in the elicitation phase significantly inhibited the neutrophil infiltration in the challenged ear and suppressed CHS.[3] Furthermore, it has been reported that corticosteroids exert their anti-inflammatory effects in contact dermatitis mainly by targeting neutrophils and macrophages.[23] These findings are consistent with our results described above and suggest that one of the anti-inflammatory effects of AE248 is through EP_3-mediated downregulation of CXCL1

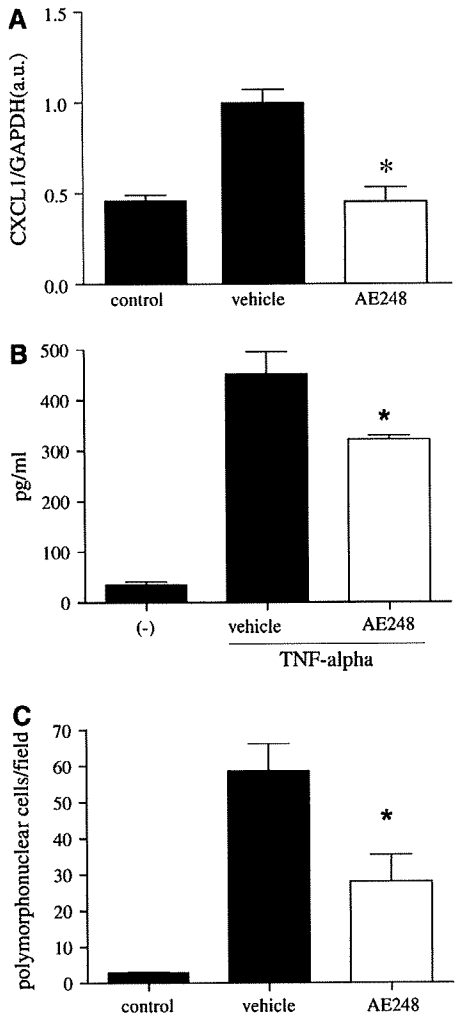

FIG 4. Effect of AE248 on CXCL1 production and neutrophil accumulation at the elicitation site. **A**, Real-time RT-PCR analysis on mRNA expression of CXCL1 in the keratinocytes in hapten-challenged ears of vehicle- or AE248-treated mice (n = 3 per group). **B**, ELISA analysis of CXCL1 production from cultured keratinocytes (n = 3 per group). Results are expressed as means ± SEMs and are representative of 3 independent experiments. **C**, Number of polymorphonuclear cells in the skin (n = 4 per group). *$P < .05$ versus the vehicle-treated group.

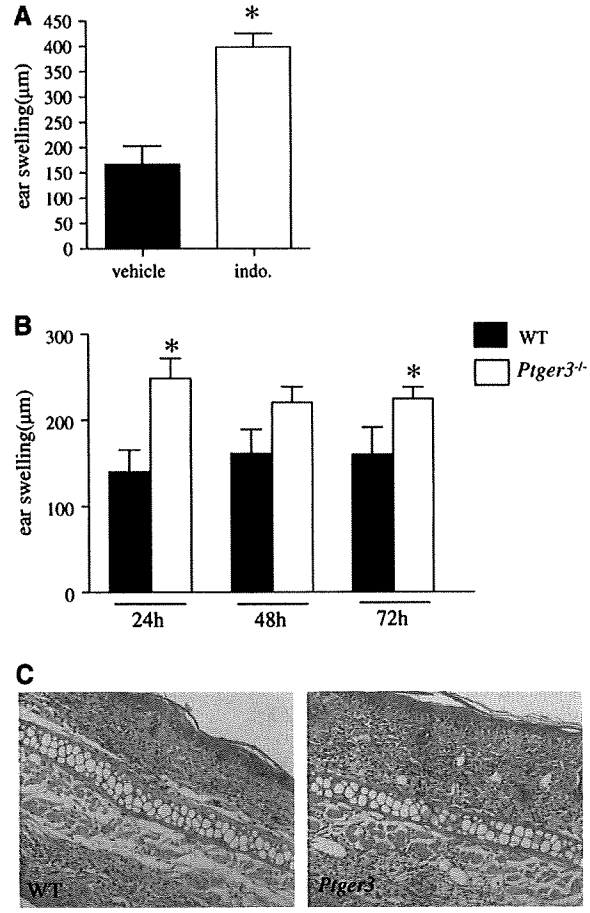

FIG 5. Enhanced inflammation of indomethacin *(indo)*-treated mice or *Ptger3*$^{-/-}$ mice in repeated-challenge CHS. **A**, Effect of topical administration of indomethacin on murine CHS (n = 4 per group). **B**, Increased ear swelling of *Ptger3*$^{-/-}$ mice in the CHS group (n = 4 per group). *$P < .05$ versus WT mice. Data are representative of 3 independent experiments. **C**, Representative HE staining of ear skin in WT and *Ptger3*$^{-/-}$ mice with repeated-challenge CHS at 24 hours after the fourth challenge.

production in keratinocytes and inhibition of neutrophil infiltration in the skin. On the other hand, our study showed that the EP_3 stimulation might have an effect on other chemokines opposite to that expected from the previous studies. For example, the expression of CCL8 was increased more than 3-fold in the AE248-treated group. In addition, we did not detect significant expression of CCL27 in our model. Given the finding that inhibition of CCL8 leads to suppression of inflammation, as described above, it is intriguing that EP_3 stimulation can reduce the inflammatory reaction in spite of such enhanced CCL8 gene expression.Unraveling this apparent discrepancy might help to reveal intricate relations among chemokines in inducing skin inflammation and define more correctly how EP_3 modulates their interaction. Taken together, chemokines from keratinocytes contribute much to the inflammation of CHS, and regulation of their production can be a useful strategy for the treatment of allergic dermatitis.

It should mentioned here that EP_3 is also expressed in mast cells in skin[24] and that mast cells can regulate the elicitation of CHS.[25,26] Indeed, expression of CXCL2 mRNA, which mast cells produce and was reported to promote neutrophil infiltration in elicitation sites, decreased to 44% of the control expression with EP_3 stimulation, although the difference was not statistically significant. However, we found that CXCL2 mRNA expression was significantly decreased in AE248-treated ears on purified keratinocytes. In addition, data of bone marrow chimera experiments indicate that most of the effect of AE248 was through stromal cells, suggesting that the anti-inflammatory effect of EP_3 derived from its action on keratinocytes.

EP_3 has 3 splice variants in the mouse, and 8 splice variants in human subjects,[27] among which at least 3 EP_3 variants are expressed in human keratinocytes.[10] They can couple Gs, Gi, and Gq and use cyclic AMP or Ca^{2+} as second messengers. EP_3 signaling can use ceramide as a second messenger in keratinocytes.[10] Our study does not clarify which signaling mechanism of EP_3 is responsible for its anti-inflammatory effect. The fact that a small dose of AE248 can induce anti-inflammatory effects is consistent with the Gi pathway because the cyclic AMP decrease mediated by Gi occurs at lower agonist

concentrations than other signaling. Indeed, the CB1 cannabinoid receptor that couples to Gi was recently reported to act on keratinocytes and suppress CHS inflammation.[28] However, this article reports that stimulation of CB1 inhibits CCL8 production from keratinocytes, which, as described, is opposite to our findings. These results indicate that multiple signaling pathways might function downstream of EP_3. It was shown recently that the Ca^{2+} signaling from EP_3 can inhibit nuclear factor κB activation in keratinocytes,[29] which is consistent with regulation of expression of CXCL1 mRNA by nuclear factor κB activity.[30] The precise molecular mechanisms underlying the anti-inflammatory effect of EP_3 remain to be elucidated.

Our results might also explain the anti-inflammatory effect of PGE_2 in skin inflammation and the adverse effect of NSAIDs in inflammatory skin diseases, such as psoriasis. Psoriasis is one of the inflammatory skin diseases, and constitutive activation of keratinocytes has been suggested as one of its causes.[21,22] Histologically, neutrophil infiltration in the epidermis is one of its characteristic features. Although PGE_2 is generally considered an inflammatory mediator by increasing vasodilation and edema formation, the anti-inflammatory effect of PGE_2 has been suggested in patients with psoriasis[31] or in animal models of neutrophil infiltration in skin.[32] On the other hand, administration of NSAIDs sometimes causes the exacerbation of psoriasis.[33,34] Thus far, the increase in levels of leukotrienes (LTs), such as LTB_4, a strong chemoattractant for neutrophils or T cells, has been suggested as one of its causative mechanisms.[33,34] Because arachidonic acid is used by both COX and lipoxygenase and NSAIDs block only COX activity, the use of NSAIDs might divert arachidonate metabolism to the lipoxygenase pathway, which leads to the increase of LTB_4. Such an argument was also made in aspirin-induced asthma. However, our study appears against such diversion mechanism. Alternatively, the PGE_2 pathway somehow modulates LT production. Our results suggest that one of the therapeutic effects of PGE_2 and an adverse effect of NSAIDs in skin inflammation is through modulation of PGE_2-EP_3 signaling.

In conclusion, stimulation of EP_3 signaling suppresses skin inflammation in CHS. Regulation of EP_3 signaling and keratinocyte function might be a novel approach for the treatment of skin inflammation, including allergy.

We thank T. Fujiwara for animal care and T. Arai for help in preparation of the manuscript.

Clinical implications: EP_3 in keratinocytes can be a target for the treatment of allergic skin inflammation.

REFERENCES

1. Grabbe S, Schwarz T. Immunoregulatory mechanisms involved in elicitation of allergic contact hypersensitivity. Immunol Today 1998;19:37-44.
2. Engeman T, Gorbachev AV, Kish DD, Fairchild RL. The intensity of neutrophil infiltration controls the number of antigen-primed CD8 T cells recruited into cutaneous antigen challenge sites. J Leukoc Biol 2004;76:941-9.
3. Dilulio NA, Engeman T, Armstrong D, Tannenbaum C, Hamilton TA, Fairchild RL. Groalpha-mediated recruitment of neutrophils is required for elicitation of contact hypersensitivity. Eur J Immunol 1999;29:3485-95.
4. Homey B, Alenius H, Muller A, Soto H, Bowman EP, Yuan W, et al. CCL27-CCR10 interactions regulate T cell-mediated skin inflammation. Nat Med 2002; 8:157-65.
5. Mitsui G, Mitsui K, Hirano T, Ohara O, Kato M, Niwano Y. Kinetic profiles of sequential gene expressions for chemokines in mice with contact hypersensitivity. Immunol Lett 2003;86:191-7.
6. Ruzicka T, Printz MP. Arachidonic acid metabolism in skin: experimental contact dermatitis in guinea pigs. Int Arch Allergy Appl Immunol 1982;69:347-52.
7. Eberhard J, Jepsen S, Albers HK, Acil Y. Quantitation of arachidonic acid metabolites in small tissue biopsies by reversed-phase high-performance liquid chromatography. Anal Biochem 2000;280:258-63.
8. Narumiya S, Sugimoto Y, Ushikubi F. Prostanoid receptors: structures, properties, and functions. Physiol Rev 1999;79:1193-226.
9. Takeshita K, Yamasaki T, Nagao K, Sugimoto H, Shichijo M, Gantner F, et al. CRTH2 is a prominent effector in contact hypersensitivity-induced neutrophil inflammation. Int Immunol 2004;16:947-59.
10. Konger RL, Brouxhon S, Partillo S, VanBuskirk J, Pentland AP. The EP3 receptor stimulates ceramide and diacylglycerol release and inhibits growth of primary keratinocytes. Exp Dermatol 2005;14:914-22.
11. Tober KL, Thomas-Ahner JM, Kusewitt DF, Oberyszyn TM. Effects of UVB on E prostanoid receptor expression in murine skin. J Invest Dermatol 2007;127: 214-21.
12. Kunikata T, Yamane H, Segi E, Matsuoka T, Sugimoto Y, Tanaka S, et al. Suppression of allergic inflammation by the prostaglandin E receptor subtype EP3. Nat Immunol 2005;6:524-31.
13. Ahluwalia A, Perretti M. Anti-inflammatory effect of prostanoids in mouse and rat skin: evidence for a role of EP3-receptors. J Pharmacol Exp Ther 1994;268: 1526-31.
14. Goulet JL, Pace AJ, Key ML, Byrum RS, Nguyen M, Tilley SL, et al. E-prostanoid-3 receptors mediate the proinflammatory actions of prostaglandin E2 in acute cutaneous inflammation. J Immunol 2004;173:1321-6.
15. Ushikubi F, Segi E, Sugimoto Y, Murata T, Matsuoka T, Kobayashi T, et al. Impaired febrile response in mice lacking the prostaglandin E receptor subtype EP3. Nature 1998;395:281-4.
16. Kabashima K, Sakata D, Nagamachi M, Miyachi Y, Inaba K, Narumiya S. Prostaglandin E2-EP4 signaling initiates skin immune responses by promoting migration and maturation of Langerhans cells. Nat Med 2003;9:744-9.
17. Ueta M, Matsuoka T, Narumiya S, Kinoshita S, Tomimatsu H, Miyauchi Y, et al. Prostaglandin E receptor subtype EP3 in conjunctival epithelium regulates late-phase reaction of experimental allergic conjunctivitis. J Allergy Clin Immunol 2009;123:466-71.
18. Honda T, Segi-Nishida E, Miyachi Y, Narumiya S. Prostacyclin-IP signaling and prostaglandin E2-EP2/EP4 signaling both mediate joint inflammation in mouse collagen-induced arthritis. J Exp Med 2006;203:325-35.
19. Latta M, Mohan K, Issekutz TB. CXCR6 is expressed on T cells in both T helper type 1 (Th1) inflammation and allergen-induced Th2 lung inflammation but is only a weak mediator of chemotaxis. Immunology 2007;121:555-64.
20. Yoo J, Omori M, Gyarmati D, Zhou B, Aye T, Brewer A, et al. Spontaneous atopic dermatitis in mice expressing an inducible thymic stromal lymphopoietin transgene specifically in the skin. J Exp Med 2005;202:541-9.
21. Sano S, Chan KS, Carbajal S, Clifford J, Peavey M, Kiguchi K, et al. Stat3 links activated keratinocytes and immunocytes required for development of psoriasis in a novel transgenic mouse model. Nat Med 2005;11:43-9.
22. Zenz R, Eferl R, Kenner L, Florin L, Hummerich L, Mehic D, et al. Psoriasis-like skin disease and arthritis caused by inducible epidermal deletion of Jun proteins. Nature 2005;437:369-75.
23. Tuckermann JP, Kleiman A, Moriggl R, Spanbroek R, Neumann A, Illing A, et al. Macrophages and neutrophils are the targets for immune suppression by glucocorticoids in contact allergy. J Clin Invest 2007;117:1381-90.
24. Nguyen M, Solle M, Audoly LP, Tilley SL, Stock JL, McNeish JD, et al. Receptors and signaling mechanisms required for prostaglandin E2-mediated regulation of mast cell degranulation and IL-6 production. J Immunol 2002;169: 4586-93.
25. Grimbaldeston MA, Nakae S, Kalesnikoff J, Tsai M, Galli SJ. Mast cell-derived interleukin 10 limits skin pathology in contact dermatitis and chronic irradiation with ultraviolet B. Nat Immunol 2007;8:1095-104.
26. Biedermann T, Kneilling M, Mailhammer R, Maier K, Sander CA, Kollias G, et al. Mast cells control neutrophil recruitment during T cell-mediated delayed-type hypersensitivity reactions through tumor necrosis factor and macrophage inflammatory protein 2. J Exp Med 2000;192:1441-52.
27. Matsuoka T, Narumiya S. Prostaglandin receptor signaling in disease. Sci World J 2007;7:1329-47.
28. Karsak M, Gaffal E, Date R, Wang-Eckhardt L, Rehnelt J, Petrosino S, et al. Attenuation of allergic contact dermatitis through the endocannabinoid system. Science 2007;316:1494-7.
29. Kanda N, Mitsui H, Watanabe S. Prostaglandin E(2) suppresses CCL27 production through EP2 and EP3 receptors in human keratinocytes. J Allergy Clin Immunol 2004;114:1403-9.
30. Scortegagna M, Cataisson C, Martin RJ, Hicklin DJ, Schreiber RD, Yuspa SH, et al. HIF-1{alpha} regulates epithelial inflammation by cell autonomous